Early life stress perturbs the maturation of microglia in the developing hippocampus

Jean-Christophe Delpech[a], **Lan Wei**[a], **Jin Hao**[a], **Xiaoqing Yu**[b], **Charlotte Madore**[c], **Oleg Butovsky**[c,d], and **Arie Kaffman**[a,*]

[a]Department of Psychiatry, Yale University School of Medicine, 300 George Street, Suite 901, New Haven, CT 06511, USA

[b]W.M. Keck Foundation Biotechnology Resource Laboratory, Yale University, New Haven, CT 06511, USA

[c]Center for Neurologic Diseases, Department of Neurology, Brigham and Women's Hospital, Harvard Medical School, Boston, MA 02115, USA

[d]Evergrande Center for Immunologic Diseases, Brigham and Women's Hospital, Harvard Medical School, Boston, USA

Abstract

Children exposed to abuse or neglect show abnormal hippocampal development and similar findings have been reported in rodent models. Using brief daily separation (BDS), a mouse model of early life stress, we previously showed that exposure to BDS impairs hippocampal function in adulthood and perturbs synaptic maturation, synaptic pruning, axonal growth and myelination in the developing hippocampus. Given that microglia are involved in these developmental processes, we tested whether BDS impairs microglial activity in the hippocampus of 14 (during BDS) and 28-day old mice (one week after BDS). We found that BDS increased the density and altered the morphology of microglia in the hippocampus of 14-day old pups, effects that were no longer present on postnatal day (PND) 28. Despite the normal cell number and morphology seen at PND28, the molecular signature of hippocampal microglia, assessed using the NanoString immune panel, was altered at both ages. We showed that during normal hippocampal development, microglia undergo significant changes between PND14 and PND28, including reduced cell density, decreased *ex vivo* phagocytic activity, and an increase in the expression of genes involved in inflammation and cell migration. However, microglia harvested from the hippocampus of 28-day old BDS mice showed an increase in phagocytic activity and reduced expression of genes that normally increase across development. Promoter analysis indicated that alteration in the transcriptional activity of PU.1, Creb1, Sp1, and RelA accounted for most of the transcriptional changes seen during normal microglia development and for most of the BDS-induced changes at PND14 and PND28. These findings are the first to demonstrate that early life stress dysregulates

*Corresponding author at: 300 George Street, Suite 901, New Haven, CT 06511, USA., arie.kaffman@yale.edu (A. Kaffman).

microglial function in the developing hippocampus and to identify key transcription factors that are likely to mediate these changes.

Keywords

1. Introduction

Abnormal hippocampal development in children exposed to abuse or neglect has been reported by several groups (Chugani et al., 2001b; Carrion et al., 2010; Maheu et al., 2010; Garrett et al., 2012; Herringa et al., 2013). Maltreated children show abnormal hippocampal activation that is associated with impaired declarative memory (Chugani et al., 2001a). Adolescents that were abused or neglected have abnormal hippocampal connectivity that is correlated with the severity of their mood and anxiety symptoms (Herringa et al., 2013). Exposure to early life stress also causes hippocampal abnormalities in nonhuman primates (Spinelli et al., 2010; Jackowski et al., 2011) and rodents (Bredy et al., 2003; Poeggel et al., 2003; Champagne et al., 2008; Ivy et al., 2010; Wei et al., 2012, 2015; Wang et al., 2013). For example, repeated maternal separation increases spine density in the hippocampus (Helmeke et al., 2001; Poeggel et al., 2003), and low levels of maternal care, early in life, are associated with reduced synaptic density in the hippocampus and poor spatial learning in adulthood (Liu et al., 2000; Bredy et al., 2003; Champagne et al., 2008).

Unfortunately, most of the animal work to date has focused on the effects of early life stress on the function and structure of the hippocampus in adulthood, with little effort made to elucidate the mechanisms by which stress early in life alters neurodevelopment (Kaffman and Krystal, 2012). To address this issue, we developed a mouse model of early life stress in which pups of the highly stress-responsive strain, Balb/cByj, are exposed to brief daily separation (BDS) during the first three weeks of life in the absence of nesting material (impoverished condition). We showed that exposure to BDS causes prolonged elevation of corticosterone in 14-day old pups and blunted the rapid increase in total DNA and RNA normally seen in the hippocampus during this age (Wei et al., 2010, 2012, 2014). Exposure to BDS was also associated with a robust increase in anxiety-like behavior and significant deficits in several hippocampal-dependent tasks in adult mice (Wei et al., 2010, 2012), consistent with the notion that BDS is a mouse model of early life stress. We have replicated these findings across multiple cohorts of Balb/cByj mice and believe that the absence of nesting material, coupled with daily separation, in this stress-reactive strain are responsible for the robust and deleterious outcomes seen in BDS mice (Wei et al., 2010, 2012, 2015). More recently, we showed that exposure to BDS impairs synaptic maturation and pruning in the hippocampus of 28-day old mice (Wei et al., 2015). Exposure to BDS also reduces the expression of proteins involved in axonal growth and myelination in the hippocampus, alterations that were detected as early as PND14 (Wei et al., 2015).

Microglia, the brain's innate immune resident cells, play a critical role in guiding many developmental processes that are affected by BDS (Wei et al., 2015). These include synaptic

pruning (Paolicelli et al., 2011; Schafer et al., 2012), synaptic maturation (Lenz et al., 2013; Parkhurst et al., 2013), neurogenesis (Butovsky et al., 2006; Wakselman et al., 2008; Cunningham et al., 2013; Ueno et al., 2013), axonal growth (Chamak et al., 1994), and myelination (Miron et al., 2013; Bhatt et al., 2014). In addition, microglia dynamically probe the developing brain and are highly responsive to several mediators of stress such as corticosterone (Wu et al., 2001; Frank et al., 2011), catecholamines (Johnson et al., 2005; McNamee et al., 2010; Wohleb et al., 2011), and corticotropin-releasing hormone (Stevens et al., 2003; Ock et al., 2006; Kritas et al., 2014). Abnormal activation of microglia has been shown to perturb several developmental processes in a manner that persists in adulthood (Schafer et al., 2012; Cunningham et al., 2013; Lenz and McCarthy, 2015). These properties led us to investigate the effects of BDS on microglia function in the developing hippocampus.

Here we show that exposure to BDS increased the density and altered the morphology of microglia in the hippocampus of 14-day old pups, effects that were no longer present at PND28. However, using the NanoString immune panel we found that BDS altered expression of many immune-related genes at both ages. We also showed that during normal hippocampal development, microglia undergo significant changes between PND14 and PND28 that include reduced cell density, decreased *ex vivo* phagocytic activity, and increased expression of genes involved in inflammation and cell migration. Hippocampal microglia isolated from 28-day old BDS mice showed an increase in phagocytic activity and reduced expression of genes that normally increase across development. Promoter analysis indicated that alteration in the transcriptional activity of PU.1, Creb1, Sp1, and RelA accounted for most of the transcriptional changes seen during normal microglia development and in response to BDS at both PND14 and PND28. These findings suggest that BDS impairs the normal maturation of microglia in the developing hippocampus and provide a possible mechanism to explain at least some of the neurodevelopmental abnormalities seen in the hippocampus of Balb/cByj mice exposed to BDS.

2. Methods

2.1. Animals

BALB/cByj mice (Stock # 001026, Jackson Laboratories) were housed in standard Plexiglas cages and kept on a standard 12:12 h light-dark cycle (lights on at 7:00 AM), at constant temperature and humidity (22 °C and 50%), with food provided *ad libitum*. The Institutional of Animal Care and Use Committee (IACUC) at Yale University approved all studies reported here.

2.2. Brief daily maternal separation (BDS)

The BDS procedure was done as described previously (Wei et al., 2010). In brief, visibly pregnant dams were placed individually in maternity cages with 750 cc of corncob bedding but no nesting material. At birth (PND = 0), pups were culled to 6–8 pups per litter, and litters were randomly assigned to either brief daily separation (BDS) or control condition. All pups were raised in the absence of nesting material, an impoverished environment that seems to contribute to the deleterious and robust effects of the BDS procedure (Wei et al.,

2010, 2012). The separation procedure occurred daily from PND1-21 and was done from 11:00 to 11:40 AM. During each BDS session, the dam was removed from the home cage and placed in a holding cage, covered with fresh corncob bedding, and provided with food and water. Pups were transferred individually into a new cage, covered with clean corncob bedding, and placed at different corners of a 20.3×27.9 cm standard cage. Cages were left undisturbed for 15 min at ambient temperature in the vivarium ($22C° \pm 2C°$) during which the pups were free to move and huddle together in their holding cage. After 15 min of separation, the pups were individually transferred back to their home cage, followed by the return of the dam. PND14 male pups were processed between 12:00 and 3:00 PM for immunohistochemistry(cell counting or morphological analysis) or fluorescence-activated cell sorting (FACS analysis) to characterize transcriptional changes and phagocytic activity. On PND 22, pups were weighed and housed in groups of 3–5 littermates of the same sex in cages with 500 cc of corncob bedding but no nesting material. On PND28, male mice were processed for immunohistochemistry and FACS analysis. Note that PND14 mice were exposed to BDS from day 1–14, while the PND28 mice were exposed to BDS from day 1–21 and then housed under normal conditions (without nesting material) until sacrifice on day 28. An independent cohort of mice was exposed to BDS and control conditions, weaned on PND22, and tested in the open field, and the elevated plus maze, at PND 35–38 (Fig. 1A).

2.3. Behavioral work

Anxiety-like behavior was tested in juvenile male mice using the open field test and the elevated plus maze (PND35-38, control n = 21, BDS n = 23–25). In the open field test, mice were allowed to explore a 50×50 cm arena for 5 min and the distance travelled and the time spent in the inner 15 cm-area were measured during the first 2 min of exploration using the EthoVision tracking system (Noldus information Technology). For the elevated plus maze, the mice were placed in the middle of a standard elevated plus maze (each arm is 10×50 cm long) facing an open arm and allowed to explore the maze for 5 min. The time spent exploring the open and closed arms, the number of entrances and the distance travelled were determined using the EthoVision tracking system.

2.4. Immunohistochemistry

All tissue was collected between 12 and 1 PM, which for PND14 pups is about 30–60 min after the pups were returned to their dam. Male mice were anesthetized with chloral hydrate (100 mg/kg) and transcardially perfused with cold PBS/heparin (50 u/ml) solution followed by 10% formalin (polyScience). Brains were then post-fixed overnight at 4 °C in 10% formalin and then equilibrated in 30% sucrose solution. Forty-micron coronal sections were collected in 6 pools, each containing 16–18 slices spaced at 240-micron intervals that systematically span the entire rostral-caudal axis of the hippocampus. One pool of slices was incubated overnight with rabbit anti Iba1 (Wako, Cat.#019-19741, 1:250) followed by biotinylated goat anti-rabbit antibodies (Vector Labs,1:250) and visualized using ABC kit (Vector Labs) and $3', 3'$di aminobenzidine (DAB) staining. Slices were then dried overnight and counterstained with Hematoxylin stain (Vector Labs).

2.5. Cell counting and morphological analysis

Unbiased stereological counting of Iba1-positive cells in the hippocampus was done using a modified version of the optical fractionator as was previously described (Wei et al., 2011). Briefly, the hippocampus borders were delineated under low magnification ($2.5 \times$) and the stereo-Investigator 10 software (MBF Bioscience) was used to determine the surface area and to count cells. All counting was done under $40 \times$ magnification by an observer who was blind to the developmental history of the mouse. The total number of Iba1-positive cells in the hippocampus was calculated as $N_{(T)} = \Sigma Q*1/ssf*1/asf*1/tsf$, where ΣQ (the total number of Iba1 cells counted, n = 500–1000 per mouse), ssf (the sampling fraction) = 1/6, asf=(area of counting frame/area of grid) = 1/9, and tsf (thickness sampling fraction) = 1. The density of microglia was calculated by dividing the total number of Iba1-positive cells counted (ΣQ.) by the total surface area of the hippocampus (in mm^2). A similar approach was used for morphological analysis, except that the asf was reduced to 1/16 and each cell was assigned to one of 4 morphological categories (e.g. amoeboid, bipolar, intermediate, and ramified). Amoeboid shape was scored for round cells with no processes, bipolar cells had only two processes and a large tear-shaped cell body, intermediate cells had multiple short processes, and ramified cells had multiple long processes. To assess Iba1 surface area, slices were coded to mask the developmental history of the mouse, and high-resolution digital images of DAB-stained slices were obtained under identical exposure conditions (Zeiss Axioplan, $10\times$ magnification). The dorsal hippocampus borders were traced and the images were analyzed with imageJ software (NIH) using the automated threshold function.

2.6. Microglia isolation from the developing hippocampus

All tissue was collected between 12 and 1 PM, which for PND14 pups is about 30–60 min after the pups were returned to their dam. To assess peripheral immune activation male mice were anesthetized with chloral hydrate (100 mg/kg) and blood was collected with EDTA-lined syringes by cardiac puncture and placed in tubes coated with 0.5 M EDTA. Mice were then transcardially perfused with 10 ml of cold HBSS buffer to remove traces of blood from the brain. Both hippocampi were then dissected, homogenized in 3 ml of cold HBSS using a glass tissue homogenizer (Kimble Chase), transferred into a 15 ml Falcon tube, and spun (280 g, 4 °C) for 7 min. Supernatant was decanted and cell pellet was resuspended in 5 ml of 70% Percoll solution layered with additional 5 ml of 37% Percoll solution. Cells were spun at 800 g for 25 min at 20 °C (brake off), and microglia-enriched fraction was collected from the 70%/37% interphase. Microglia-enriched fraction was then washed with 10 ml of cold FACS buffer (0.2% BSA in HBSS), and spun at 280 g for 7 min at 4 °C. The supernatant was removed and the cell pellet was resuspended in 300 μL of cold FACS buffer and blocked with rat- anti CD16/CD32 Fc antibodies (Cat# 553142, BD Biosciences, 1:100) for 10 min on ice. Microglia were then stained with rat-anti CD11b-PeCy7 antibodies (Cat# 25-0112-82, ebiosciences, 1:100) and rat-anti CD45-PeCPCy5.5 antibodies (Cat# 45-; 0451-82, ebiosciences, 1:100) for 25 min on ice. Labeled cells were washed with 3 ml of cold FACS buffer, spun as above, resuspended in 300ul of cold FACS buffer and FACS sorted using a BD FACSAria™ II flow cytometer (BdBiosciences). Microglia were collected directly in a tube containing 300 μL of mirVana lysis buffer, frozen in liquid nitrogen, and stored at −80 °C.

2.7. Peripheral immune activation

Whole blood was collected as described in Section 2.6 above. Red blood cells were lysed and the samples were washed and blocked with rat anti CD16/CD32 antibodies. Cells were washed again and then incubated with rat anti-CD11b PE-Cy7 (Cat# 25-0112-82, eBioscience, 1:500) and rat anti-Ly6C FITC, (Cat # 553104, BD Biosciences, 1:1000) for 30 min at RT. Cells were then washed, resuspended in FACS buffer, and assessed for antigen expression using a BD LSRfortessa FACS (BD Biosciences). Data were analyzed using FlowJo software (Tree Star) and gating for each antibody was determined with isotype stained control.

2.8. Western blot

Eight microliters of plasma were loaded per lane and separated on a 12% Criterion™ TXG Stain Free midi-gel (cat* 567-8044, BioRad) followed by a 1-min UV-activation using the ChemiDoc XRST imaging system (Bio-Rad). Proteins were then transferred to a nitrocellulose membrane (Cat#l70-4159, Bio-Rad) via the trans-Blot® Turbo system (Bio-Rad), and total protein load in each lane was quantified using the ChemiDoc XRST imaging system (see bottom panels in Fig. 4). Membranes were subsequently blocked for 60 min at RT in 5% Omniblock (in PBS with 0.1% Tween-20), and incubated with goat anti CRP antibodies (1:200, Santa Cruz, Cat# sc-18304) at 4 °C overnight with gentle shaking. Membranes were washed with PBS containing 0.1% Tween-20 and incubated with horse anti goat secondary antibodies conjugated with HRP for 1hr at RT. Proteins were detected using Western Lightning® Western Blot Chemiluminescence Reagent Plus kit (NEL104001EA, PerkinElmer), quantified using the ChemiDoc XRST imaging system, and normalized to membrane load (Eaton et al., 2013).

2.9. RNA isolation and NanoString nCounter analysis

Total RNA was isolated from microglia using the mirVana mirRNA isolation kit (Cat # AM 1560, Life technologies) and was then concentrated and DNase treated on column using the RNA clean and contractor-5 kit (Cat# R1015, Zymo Research). RNA quality was assessed using Agilent RNA 6000 pico Kit (Cat# 5067-1514 Agilent Technologies) and quantified using q-PCR against a standard curve made with known amounts of purified RNA. For Nano-String gene analysis, 2 ng of RNA were converted to cDNA using SuperScript VILO (Cat# 11754, Life Technologies), amplified with 5 rounds of PCR according to the nCounter single cell gene expression protocol and hybridized to the mouse immune panel (Cat# 150761, NanoString Technologies) according to manufacturer instructions. Counts were normalized to positive controls and 6 housekeeping genes (e.g. Alas1, Gapdh, Oaz1, Polr1b, Sdha, Tbp). These housekeeping genes were selected because they were not affected by either BDS or age and showed a coefficient of variation of less than 20%. Genes were considered "present" if at least 40% of the samples showed hybridization signal that was 2 s.d. above the mean value for the negative control probes. All data, including raw counts, were deposited and are available at GEO archive accession # GSE81038.

2.10. Q-PCR validation

cDNA was synthesized using 1–2 ng of total RNA per sample using SuperScript VILO (Cat# 11754, Life Technologies). Q-PCR was performed using QuantiTect-SyBr Green (Qiagen, Cat# 204143) and analyzed on a 96-well, Stratagene Mx3000 thermocycler in triplicates using a list of primers shown in Table S4. Efficiency of all primers was confirmed to be $100 \pm 10\%$ and the $2^{-\Delta\Delta CT}$ method was used (Pfaffl, 2001) to calculate relative RNA levels, with Oaz1 as an internal housekeeping gene and the control group used as the calibrator.

2.11. Lipopolysaccharide (LPS) injection

Eight-weeks old Balb/cByj mice were injected with LPS (*Escherichia coli* 011:B4, Sigma Chemical Co.) or saline i.p. (n = 4 in each group). Twenty hours later microglia were isolated from the hippocampus and RNA was extracted and processed for q-PCR as described in Sections 2.5,2.7 and 2.8 respectively.

2.12. Ex-vivo phagocytic assay

The *ex-vivo* phagocytic assay was adapted from previously published protocols (Paresce et al., 1996), with the following modifications. PHrodo Green *E. Coli* bioparticles (Cat# P35366, Life Technologies) were resuspended in 200uL of sterile PBS, sonicated, and opsonized using rabbit anti-*E. Coli* IgG antibodies (Cat# E2870, Life Technologies). Microglia were purified from the developing hippocampus using a Percoll gradient (Section 2.5), washed with RPMI/1% BSA buffer, and divided into three 100uL aliquots each containing 2.5×10^5 microglia. Each aliquot was incubated with 20 μL of opsonized pHrodo *E. Coli* bioparticles (3×10^5 bioparticles/μL) at 37 °C and 5% of CO_2. Reactions were stopped at different time points (0, 30, and 60 min) by the addition of cold RPMI/1% BSA buffer and placed on ice. Cells were then pelleted at 1000 g for 10min at 4 °C, resuspended in 200 μL of RPMI/1%BSA buffer, stained with CD11b-PE Cy7 and CD45-PeCPCy5.5 antibodies and processed for FACS analysis as described in Section 2.6 except that the t = 0 time point was used to determine appropriate gating.

2.13. Statistical analysis

Data were carefully screened for inaccuracies, outliers, normality and homogeneity of variance. A two-way ANOVA was used to assess the effects of BDS and age on weight, hippocampal volume, number of microglia, microglia density, Iba1 surface area, morphological analysis, FACS analysis, CRP levels, and phagocytic activity. Significant effects were followed by Bonferroni-corrected *post-hoc* analyses. Unpaired Student t-tests were used to assess the effect of BDS on behavior and gene expression with $p < 0.05$ (two tails) considered significant. Promoter analysis was done using the network-building algorithm for transcription regulation in the MetaCore software (Thomson Reuters) with p-value and enrichment for each transcription factor calculated based on hypergeometric distribution. Transcription factors with Benjamini–Hochberg Multiple Testing Correction p-value of ≤0.05 were considered significant. The MeteCoreGeneGO server (https://portal.genego.com/) was used to conduct pathway analysis based on pathway, biological functions, and GO biological processes of differentially expressed genes. P-values were

calculated based on hypergeometric distribution to assess the probability for a pathway to arise by chance. Pathways and networks with a Benjamini–Hochberg Multiple Testing Correction p-value of ≤0.05 were considered significant.

3. Results

3.1. BDS increases anxiety-like behavior in juvenile mice

We have previously shown that exposure to BDS increases anxiety-like behavior in adulthood (Wei et al., 2010, 2012). However, the effects of BDS on these behaviors in juvenile mice have not been examined yet. To address this issue, we tested two anxiety-like behaviors (e.g. open field and elevated plus maze) in juvenile mice that were raised under control or BDS condition (See Fig. 1A for timeline). We focused on male mice because our previous work (Wei et al., 2010, 2012) and work from other laboratories, showed that the effects of early life stress on neurodevelopment and behavior are more robust in male mice (Loi et al., 2015). We found that juvenile BDS mice spent less time exploring the center of the open field ($t_{(42)} = 2.2$, $p < 0.05$, Fig. 1B) and entered fewer times into the center of the arena compared to controls ($t_{(42)} = 2.6$, $p < 0.05$, Fig. 1C). BDS did not affect the overall distance travelled in the arena (Fig. 1D), indicating that it does not affect overall locomotor activity. Mice exposed to BDS also spent less time ($t_{(44)} = 2.4$, $p < 0.05$, Fig. 1E), and entered fewer times into the open arms ($t_{(44)} = 2.0$, $p = 0.05$, Fig. 1F). BDS did not affect the total distance travelled in the elevated maze (Fig. 1G), or time spent in the less anxiogenic closed arms (Fig. 1H), but there was a trend for increased entries into the closed arms ($t_{(44)} = 1.9$, $p = 0.07$, Fig. 1I). These findings indicate that exposure to BDS increases anxiety-like behavior in juvenile mice.

3.2. BDS increases the number of microglia in the hippocampus of PND14, but not PND28 mice

Given that microglia regulate many of the developmental processes that are impaired in BDS mice, we first tested the effects of BDS on the number of these cells in the hippocampus of PND14 and PND28 male offspring (see Fig. 1A for timeline). We chose PND14 because the number and density of microglia peak in the hippocampus at this age (Paolicelli et al., 2011). PND28 was selected because it is characterized by intense synaptic pruning in the hippocampus (Steward and Falk, 1991; Dalmau et al., 1998; Faulkner et al., 2007) and because BDS impairs synaptic maturation and pruning at this age (Wei et al., 2015).

Both control and BDS mice showed a significant increase in weight ($F(1,30) = 253.92$, $p < 0.001$, Fig. S1A), and hippocampus volume with age ($F(1,30) = 23.6$, $p < 0.001$, Fig. S1B). There was a trend for reduced weight in BDS mice ($F(1,30) = 2.97$, $p = 0.09$, Fig. S1A), but no effect of BDS on hippocampus volume (Fig. S1B). Inspection of hippocampal slices stained with anti-Iba1 antibodies suggested that both age and BDS affected microglia number and morphology (Fig. 2A). Using unbiased stereology we found a significant reduction in the total number of microglia in the hippocampus of 28-day old male mice ($F(1,30) = 16.17$, $p < 0.0005$, Fig. S1C), and a significant effect of BDS ($F(1,30) = 4.82$, $p < 0.05$, Fig. S1C). There was a trend for the interaction ($F(1,30) = 2.81$, $p = 0.104$) that was due to increased microglia number in the hippocampus of 14-day old BDS pups (Fig. S1C).

Using microglia density as a combined measure of hippocampus volume and total cell number we found a significant effects of age ($F_{(1,29)} = 163.7$, $p < 0.001$, Fig. 2B), BDS ($F_{(1,29)} = 8.33$, $p < 0.01$, Fig. 2B), and an interaction ($F_{(1,29)} = 6.80$, $p < 0.05$, Fig. 2B). Post-hoc analysis revealed that BDS increased cell density at PND14 ($p < 0.05$), but not PND28 (Fig. 2B).

To characterize the effects of age and BDS on microglia morphology we measured the surface area of all Iba1-positive cells in the hippocampus. We found significant effects of age ($F_{(1,28)} = 1451$, $p < 0.0005$, Fig. 2C), BDS ($F_{(1,28)} = 7.53$, $p < 0.05$, Fig. 2C), and an interaction ($F_{(1,28)} = 6.75$, $p < 0.05$, Fig. 2C). Post-hoc analysis showed that BDS increased microglia surface area in 14-day old BDS mice ($p < 0.05$), an effect that did not persist in 28-day old BDS mice (Fig. 2C). Next, we assigned each microglia to one of four morphologies: amoeboid, intermediate, bipolar, and ramified cells (Fig. 2D–G). Amoeboid and intermediate cells showed similar patterns with no significant effects of age or BDS but significant interactions (amoeboid: $F_{(1,28)} = 13.69$, $p < 0.001$, Fig. 2D; intermediate: $F_{(1,29)} = 9.12$, $p < 0.01$, Fig. 2E) that were due to significant increase in the number of these cells at PND14 ($p < 0.05$), but not PND28 (Fig. 2D, E). Bipolar cells showed a significant effect of age ($F_{(1,29)} = 254.8$, $p < 0.001$, Fig. 2F), BDS ($F_{(1,29)} = 23.7$, $p < 0.0001$, Fig. 2F), and an interaction ($F_{(1,29)} = 18.76$, $p < 0.0001$, Fig. 2F), with *post-hoc* analysis showing a significant increase in the number of bipolar cells in BDS mice at PND14 but not at PND28 (Fig. 2F). Finally, the ramified microglia, representing the vast majority of the microglia in the hippocampus showed a significant effect of age ($F_{(1,30)} = 15.37$, $p < 0.001$, Fig. 2G), a trend for a BDS effect ($F_{(1,30)} = 2.89$, $p = 0.099$, Fig. 2G), and no interaction (Fig. 2G). Together, these findings are the first to show that early life stress increases the density of microglia in the hippocampus of PND14 male pups. This effect was more pronounced in microglia with simplified morphologies (i.e. amoeboid, intermediate, bipolar) and was not seen on PND28 when the density of microglia is significantly lower.

3.3. Exposure to BDS increases the number of CD11b-positive cells in the blood of PND14, but not PND28 mice

Microglia activation in the brain has been tightly linked to peripheral immune activation in some forms of stress (Wohleb et al., 2011, 2013, 2014). We thus characterized the effect of BDS on the levels of CD11b-positive cells, CD11b/SSC^{hi}/Ly6C^{int} (granulocytes), and CD11b/SSC^{low}/Ly6C^{hi} (monocytes) in the blood of PND14 and PND28 male pups (Fig. 3A). We found a significant interaction between BDS and age on the number of CD11b-positive cells ($F_{(1,25)} = 4.40$, $p < 0.05$, Fig. 3B). Post-hoc analysis showed a significant increase in the number of these cells at PND14, but not at PND28 (Fig. 3B). This transient increase in CD11b-positive cells appeared to be driven by an increase in CD11b/SSC^{hi}/Ly6C^{int} granulocytes at PND14 (Fig. 3C), but not CD11b/SSC^{low}/Ly6C^{hi} monocytes (Fig. 3D). Together, these findings indicate that concomitant with the effect on microglia in the hippocampus, BDS causes peripheral immune activation in 14-day old male pups, an effect that is no longer present at PND28.

One of the most robust peripheral immune markers associated with childhood maltreatment is elevated level of the acute phase reactant c-reactive protein; elevated levels that in many

cases persist into adulthood (Coelho et al., 2014). We therefore asked whether exposure to BDS increases levels of c-reactive protein (CRP) in the plasma of PND14 (Fig. 4A) and PND28 mice (Fig. 4B). We found a significant effect of age $F(1,26) = 19.9$, $p<0.0005$, BDS $F(1,26)= 16.9$, $p < 0.0005$, and a trend for the interaction $F (1,26) = 3.28$, $p = 0.082$ (Fig. 4C). These findings demonstrate that some immune markers continue to be elevated in BDS mice even in the absence of on going stress.

To test whether peripheral immune activation was associated with increased infiltration of blood monocytes into the brain (Wohleb et al., 2013), we quantify the number of CD11b/CD45^{high} brain macrophages from the developing hippocampus (Fig. S2A). We found a significant effect of age ($F(1,32) = 34.4$, $p< 0.0005$, Fig. S2B), but no effect of BDS or interaction on the number of CD11b/CD45^{high} brain macrophages in the hippocampus (Fig. S2B). These finding suggests that peripheral immune activation is not associated with infiltration of macrophages in the developing hippocampus of PND14 BDS mice.

3.4. Microglial molecular signature is dysregulated in the hippocampus of 14-day old BDS mice

To further characterize the effects of BDS and age on microglial gene expression we adopted a previously reported protocol (Butovsky et al., 2014) to isolate microglia (CD11b/CD45^{int} cells) from the developing hippocampus of a single pup. RNA extracted from these cells is highly intact (RIN > 9) and is enriched for microglial-specific-genes (Fig. S2C). Microglia isolated using this procedure showed a significant induction of IL1b (Fig. S2D) and other cytokines (data not shown) in response to in vivo LPS administration (see methods, Section 2.9 for details), indicating that this procedure can be used to distinguish between "activated" and "non-activated" microglia.

Next, we used the NanoString mouse immune chip to characterize the effect of BDS on the expression of 545 key immune-related genes in microglia isolated from the hippocampus of 14-day old pups. Of the 286 genes detected by the panel, 58 genes showed significant dysregulation by BDS at this age (Fig. 5A), with 33 genes showing down regulation, and 25 genes showing a significant upregulation (Fig. 5B and C). Using q-PCR we confirmed differential expression of 7 out of the 9 genes tested (Fig. 5D), demonstrating that the immune panel provides a reliable method to identify changes in gene expression. Pathway analysis (Fig. 5E) indicated that BDS altered expression of genes involved in cell cycle regulation and apoptosis (e.g. Csf1, Csf3r, Beta catenin, Tgfbr2, Cd81, Casp2, Casp8, Fig. 5A and Table S1), providing a possible mechanism to explain the increase in the number of microglia seen at this age. BDS increased levels of genes that mediate microglial activation such as Fyn, Irak4, Tbk1, and Chuck while at the same time reduced expression of several pro-inflammatory genes including IL1a, IL1r1, CD40-ligand, Tlr9, Mif, Ifnar2, Ifnrg1, RelA, Traf3, and increased levels of anti-inflammatory genes such as ILlOrb, Cd83, and Jak3 (Fig. 5A and Table S1). This complex immune response was not associated with increased levels of IL-1β, Tnf-α, IL-6 or IL-10 (Fig. 5A and Table S1), indicating that BDS did not induce classical immune activation in microglia isolated from the hippocampus on PND14. Exposure to BDS also modified expression of genes implicated in cell migration

(e.g. Ccl4, Ccr6, Ccr2, Cxcr6, Cx3cr1 Itga5, Itgb1) and several phagocytosis-related genes, including Itgam/Cd11b, C1qa, C1qb and Cfh (Fig. 5A and Table S1).

To identify the transcription factors responsible for this immune profile, we conducted a promoter analysis using the Meta-Core software. This analysis indicated that the transcription factor cAMP response element binding protein 1 (Creb1) accounted for 71% (p = 5.96e^{-139}) of the 58 genes that were regulated by BDS. The transcription factors Sp1 and RelA (a subunit of the NFKB transcription factor) were also highly enriched accounting for 57% (p = 1.73e^{-110}) and 55% (p = 1.67e^{-108}) of the genes regulated by BDS at this age (Fig. 5F). These 3 transcription-factors combined accounted for 76% of the genes regulated by BDS at PND14, sharing a significant overlap in the target genes they modified (Table S1). The Nanostring panel does not contain probes for Creb1 and Sp1, but it does contain a probe for RelA which showed reduced RelA levels in microglia isolated from the hippocampus of 14-day old BDS mice (Table S1). Together, these findings suggest that BDS alters microglial gene expression profile at PND14 in the hippocampus by modifying the activity of Creb1, SP1, and RelA.

3.5. BDS alters gene expression in microglia isolated from the hippocampus of PND28 mice

Although, BDS did not affect the number and morphology of microglia on PND28 (Fig. 2), some of the transcriptional changes seen at PND14 may have persisted at this later age. To assess this, microglia were isolated from the hippocampus of 28-day old control and BDS mice. Of the 364 genes detected at this age, 35 genes were down regulated and only 8 genes (Blnk, Cd24a, Ccl9, Ebi3, H2-Ea-ps, Foxp3, Tnfrsf13b, IL-6) were upregulated (Fig. 6A–C). Pathway analysis (Fig. 6D) indicated that BDS reduced expression of many pro-inflammatory genes such as Lck, Tlr3, Tlr5, Tlr9, IL17ra, Notch1, Stat1, and Stat5 (Fig. 6A and Table S2). BDS was also associated with reduced levels of several chemotaxis-related genes, such as Cdh5, Cmklr1, Cd164, Gpr183, Ccr6, Ccl9 and Itgb1 (Fig. 6A and Table S2). Although the overall pattern suggested an anti-inflammatory response, BDS also increased levels of several pro-inflammatory genes, including IL-6, Tnfrsf13b, Ebi3, and reduced expression of anti-inflammatory genes such as Il4ra and Maf (Fig. 6A and Table S2). These findings are consistent with the notion that BDS causes a complex immune response. When we compared the effect of BDS on PND14 and 28 we found that ten of the 43 genes regulated by BDS at PND28 were also regulated at PND14 (Fig. 6E). Four of these genes (Csf1, Ptprc, Itgb1, Cmklr1) were down regulated on PND14 but significantly upregulated on PND28, suggesting a possible rebound effect. The remaining 6 genes (Adal, Ccr6, Ski, Maf, Tgfbr2, Tlr9) were down regulated at both ages, demonstrating that BDS causes long-term alteration in the expression of some genes in microglia. Similar to our findings at PND14, promoter analysis indicated that alterations in Creb1, Sp1, PU.1 and RelA transcriptional activities accounted for 86% of the genes regulated by BDS at PND28 (Fig. 6F). Whereas microglia morphology did not reveal any microglia alteration at PND28, gene expression profile suggested that effects of BDS persist in microglia in the hippocampus of 28-day old mice by altering the activities of Creb1, Sp1, RelA and PU.1 in these cells.

3.6. Levels of phagocytic activity decrease with age in control, but not in BDS mice

Our genomic data suggested that BDS might alter phagocytic activity in microglia located in the developing hippocampus (Fig. 5E and 6D). To further assess this we developed an *ex vivo* phagocytic assay. Microglia were acutely isolated from the hippocampus on PND14 and PND28 and incubated with opsonized *E. Coli* conjugated-PH-sensitive fluorescent bio-particles to test their FC-dependent phagocytic activity. The fluorescence intensity of these bio-particles increases when they enter the acidic environment found in microglial lysosomes (Takenouchi et al., 2009; Ghosh and Geahlen, 2015) and therefore the phagocytic rate can by determined by using FACS to monitor the increase in fluorescence intensity as a function of time (Fig. 7A). We found that BDS had no effect on the phagocytic activity at PND14 ($F(1,70) = 2.54$, $p = 0.11$, Fig. 7B), but increased phagocytic activity at PND28 ($F(1,42) = 9.49$, $p<0.01$, Fig. 7C). To further characterize the effects of Age and BDS we used the area under the curve (AUC) as the summation of phagocytic activity. Using this analysis we found a main effect of age ($F(1,35) = 11.05$, $p < 0.01$, Fig. 7D), and a trend for an interaction ($F(1,35) = 3.42$, $p = 0.07$, Fig. 7D). Post-hoc analysis showed a significant reduction in phagocytic activity in PND28 control, but not BDS mice (Fig. 7D). These findings demonstrate that levels of phagocytic activity decrease with age in control mice, but not in BDS mice where the phagocytic activity at PND28 is maintained at levels normally seen at PND14.

3.7. BDS perturbs the maturation of microglia in the juvenile hippocampus

Microglia undergo significant changes in density, surface area, morphology, and phagocytic activity during the third and fourth weeks of hippocampal development (Figs. 2 and 7). To further characterize these developmental changes, we identified a list of 76 genes whose expression was altered in microglia harvested from the hippocampus of PND14 and PND28 control animals (Fig. 8A, B). This list included genes that showed significant change across development in two independent cohorts (Table S3). Only 3 genes were upregulated at PND14 compared to PND28 (Ebi3, Cd79b, Fcgrt), and 73 genes showed a significant increase with age (Fig. 8C, Table S3). Pathway analysis indicated that most of the genes that were regulated by age were implicated in immune modulation (41%), cell migration (16%), and antigen presentation (12%), with relatively few genes involved in phagocytosis (4%) or cell cycle regulation (6%). Interestingly, 13 of the 35 genes that were down regulated by BDS at PND28 were developmentally regulated (Fig. 8D). Promoter analysis showed that the transcription factors PU.1, c-Myc, Sp1, RelA, and Creb1 played an important role in normal microglia development (Fig. 8E). Given that the transcription factor PU.1 plays a critical role in the development and function of microglia (Yeamans et al., 2007; Feng et al., 2008; Kierdorf et al., 2013; Smith et al., 2013), we used q-PCR to test the effects of age and BDS on mRNA levels of PU.1. Consistent with our promoter analysis, we found a significant effect of age ($F(1,31) = 56.9$, $p < 0.0005$, Fig. 8F) that was due to a 60% increase in levels on PND28. There was also a significant effect of BDS ($F(1,31) = 6.79$, $p = 0.015$, Fig. 8F), due to 15–20% reduction seen on PND14 and PND28, with no significant interaction. Together with our *ex vivo* phagocytic assay, these findings suggest that BDS interferes with the normal maturation of microglia in the juvenile hippocampus by disrupting the activity of several transcription factors including PU.1, RelA, Creb1 and Sp1.

4. Discussion

Exposure to BDS recapitulates several clinical findings reported in maltreated children, suggesting good construct validity as a model of childhood adversity. These include: elevated corticosterone levels during the postnatal period, abnormal hippocampal development, and reduced myelination (Wei et al., 2010, 2012, 2014, 2015). In this report we show that the increase in anxiety-like behaviors, previously reported in adult BDS mice (Wei et al., 2010, 2012), can also be detected during the juvenile period. Moreover, the ability of BDS to induce significant peripheral immune activation and to increase CRP levels are also consistent with a large body of work showing elevated immune response in maltreated children (Coelho et al., 2014). This issue is particularly interesting given that abnormal RelA activity reported here in microglia was also observed in peripheral immune cells harvested from woman exposed to childhood maltreatment (Pace et al., 2012). Several technical features that are unique to our BDS procedure (i.e. the absence of nesting material, the spreading of pups in the separation cage, and the stress reactivity of the Balb/cByj strain) are likely responsible for the robust but diametric opposing outcomes seen in BDS mice compared to those previously reported after brief handling in rat pups (Levine et al., 1967; Hess et al., 1969; Meaney et al., 1989; Wei et al., 2010, 2012).

The unique ability of microglia to dynamically probe the brain parenchyma makes them highly sensitive sensors of environmental changes, including stress (Kaur et al., 1994; Wu et al., 2001; Frank et al., 2011; Wohleb et al., 2011). Alteration in microglial activity during critical periods of development has been shown to modify a host of developmental processes in a manner that persists in adulthood (Schafer et al., 2012; Cunningham et al., 2013; Lenz and McCarthy, 2015). These observations inspired several groups to investigate the effects of early life stress on microglial function in the developing (Gomez-Gonzalez and Escobar, 2010; Bolton et al., 2013; Roque et al., 2015) and adult brain (Bilbo et al., 2007; Diz-Chaves et al., 2012, 2013; Takatsuru et al., 2015). The only previous study that examined the effects of postnatal stress on immune activation in the developing hippocampus found similar morphological changes in microglia after 3hrs of daily maternal separation in 14-day old rat pups (Roque et al., 2015), indicating that this is not a unique feature of our paradigm. These authors did not find an increase in the density of microglia at this age, probably due to the fact that they examined this issue only in the hilus of the dentate gyrus versus the entire hippocampus as was done here. Our study extends these initial findings by characterizing the effects of BDS on microglia cell number, morphology, transcriptome and *ex vivo* phagocytic activity at PND14, during the BDS period when the number and density of microglia in the hippocampus reaches a developmental peak (Dalmau et al., 1998; Paolicelli et al., 2011) and at PND28, one week after the last exposure to BDS, when BDS perturbs synaptic pruning, myelination, and axonal growth (Wei et al., 2015).

We confirmed previous findings showing that the density of microglia in the hippocampus declines between PND14 and PND28 (Paolicelli et al., 2011). Two parallel processes drive this developmental change. First, the total hippocampal volume increases by roughly 50% during these two weeks. Second, the number of microglia is reduced during these two weeks by roughly 30% via a mechanism that has not yet been described. Given that microglia are evenly distributed in the hippocampus, the relative territory monitored by each cell increases

by almost 3-fold during these 2 weeks. We found that this increase in territory is associated with reduced *ex vivo* phagocytic activity and an increase in genes involved in inflammation (e.g. RelA, IL-1b, IL-1a, Tlr4, Trl3, Icos-ligand) cell migration (e.g. Ccr6, Ccl6, Ccl24, Pdgfb, Pdgfrb, Gp1183), and antigen presentation (H2-DMa, H2-Ob, Xb1, Cd74, see Table S3). Based on our promoter analysis, we propose that microglia undergo a maturation process that is guided by the transcriptional activation of PU.1, c-myc, RelA, Sp1 and Creb1. This maturation process leads to the selection of a sub-population of competent microglia that are necessary to support the rapid synaptic maturation, axonal growth, and the increase in myelination seen in the hippocampus during these two weeks of development (Wei et al., 2015).

Exposure to BDS caused a significant increase in the number, density, and surface area of microglia at PND14, effects that did not persist at PND28. To better understand the molecular mechanisms by which BDS modifies microglia, we examined the effect of BDS on gene expression in microglia isolated from the hippocampus of 14-day old pups. Using this approach we found that BDS increased expression of many genes that regulate cell-cycle progression and survival (Fig. 5 and Table S1), including the colony stimulating factor 1 (Csf1), a cytokine that has been shown to play a critical role in microglial proliferation and survival (Erblich et al., 2011; Rice et al., 2015). BDS also increased the expression of several genes involved in apoptosis (e.g. Casp2, Casp8) and reduced the expression of genes known to drive cell cycle progression (Beta catenin/Ctnbb1, Tgbfbr2, Csf3r, RelA). These changes may help restrict the extent of microgliosis seen in the hippocampus of 14-day old pups and help restore the normal number of microglial cells at PND28.

Microglia isolated from the hippocampus on PND14 showed an alteration in the expression of genes known to affect cell migration (e.g. Ccl4, Ccr6, Ccr2, Cxcr6, Cx3cr1 Itga5, Itgb1) and phagocytosis (e.g. Itgam/Cd11b, C1qa, C1qb, Cfh). However, BDS did not alter the *ex vivo* phagocytic activity in microglia isolated from the hippocampus on PND14. This result needs to be interpreted with caution given recent work showing that a high-fat diet increases phagocytic activity when microglial cells are incubated with synaptosome-conjugated, but not *E. coli* coated, fluorescent bio-particles (Hao et al., 2016). Additional work is therefore needed to test the effect of BDS on phagocytic activity towards more relevant substrates such as synaptosomes, neural stem cells, myelin, or axonal segments. Even in the absence of an effect on the phagocytic rate, the higher number of these cells suggests an overall increase in phagocytic capacity in the hippocampus of 14-days old BDS pups. Such enhanced capacity may explain the reduced axonal growth and myelination seen at this age in the hippocampus (Wei et al., 2015).

The effects of BDS on microglial function in the hippocampus persisted in 28-day old juvenile mice. These effects include the reduction in levels of genes involved in immune activation and chemotaxis and an increase in the phagocytic activity. The mechanisms by which BDS increases the phagocytic activity of microglia is unclear at this point, but it might be related to the number of exposures to BDS (14 vs. 21 days, see Fig. 1A for timeline). In addition, it is possible that the ability of BDS to increase corticosterone in the pups, a process that starts only after PND14 (Wei et al., 2010, 2012) and has been associated with increased phagocytic activity (Bellavance and Rivest, 2014) is responsible for the

delayed effect of BDS on phagocytic activity. Future work will test whether microglia-specific deletion of the glucocorticoid receptor can block the anti-inflammatory expression profile and the increase in the phagocytic rate seen in 28-day old BDS mice. Additional work is also needed to clarify whether some of the transcriptional changes seen at PND28 are still present in adulthood and whether they sensitize the microglial response to stress in adulthood.

The number and the morphology of microglia were not altered in the hippocampus of 28-day old BDS mice, underscoring the limitation of these approaches to identify more subtle changes in microglia function. BDS reduced expression of several developmental genes including PU.1, Tgfbr2, Stat5a, Ccr6, and Tlr9, Gpr183, Ptprc, suggesting that BDS interferes with the normal maturation of these cells. This assertion is also supported by the high phagocytic activity seen in microglia isolated from the hippocampus of PND28 BDS mice. Using promoter analysis we found that alteration in the activity of Creb1, Sp1, and RelA accounted for 76% and 86% of the transcriptional changes seen in microglia isolated from the hippocampus of 14 and 28-day old mice respectively. These three transcription factors showed significant overlap in their transcriptional targets (Tables S1 and S3), suggesting that they may interact to orchestrate the effects of BDS on microglia. Though these transcription factors are known to play a critical role in mediating many immune functions including cell cycle progression, cytokine production, cell migration, phagocytosis, and cellular differentiation (Roy et al., 2006; Wen et al., 2010; Park et al., 2015), their role in guiding microglial function in the developing brain has not been studied. It will be of great interest to test whether a microglia-specific deletion of PU.1 or RelA during the second week of life is sufficient to recapitulate some of the developmental and behavioral changes seen in BDS mice. Such work will allow us to address the question of whether the changes in microglia reported here represent a compensatory mechanism that minimizes the deleterious effects of BDS or whether these changes actively contribute to the developmental and behavioral abnormalities seen in BDS mice (Wei et al., 2010, 2012, 2015).

BDS also activates the immune response in the periphery as seen by the increase in the number of CD11b-positive cells and the proportion of CD11b/SSC^{hi}/Ly6C^{int} granulocytes in blood collected from 14-day old pups. In addition, BDS mice showed an increase in plasma CRP levels at PND14, an effect that was even more pronounced at PND28 (Fig. 4). These findings are consistent with work from several groups showing that childhood maltreatment is associated with increased peripheral immune activation in adults and children (Coelho et al., 2014). This is interesting because of an emerging body of work showing that peripheral immune activation plays an important role in modifying microglial activity and behavior (Wohleb et al., 2013, 2014; Hodes et al., 2014). For example, exposure to social defeat causes the recruitment of peripheral monocytes into the brain parenchyma where they are referred to as brain macrophages. This recruitment process is necessary to activate microglia and to increase anxiety-like behavior in socially defeated mice (Wohleb et al., 2013). Despite the fact that BDS causes significant peripheral immune activation, it does not increase the number of macrophages in the hippocampus. This might be due to genetic and immunological differences between Balb/cByj used here and the C57 strain used in the social defeat work, or differences in the developmental state of the animal (PND14 vs.

adulthood), and/or the nature of the stressor (BDS vs. repeated social defeat). Nevertheless, it will be interesting to test whether BDS causes an increase in cytokine levels in the periphery and whether this increase is necessary to activate microglia in the developing hippocampus of the pups. It will be important to clarify whether BDS increases immune activation in the dams and whether cytokines induced in the dams can trigger an immune response in the pups via lactation. This possibility is particularly intriguing given the role that cytokines present in breast milk play in mediating immune responses early in development (Garofalo, 2010).

In summary, work presented here provides four novel insights into the mechanisms by which BDS modifies microglia function during a critical period of hippocampal development. First, this is the first study to show that exposure to postnatal stress increases the density of microglia in the hippocampus of 14-day old pups. Second, we found that this increase in microglia number is associated with changes in the expression of many genes involved in cell cycle progression, inflammation, and cell migration. Third, promoter analysis indicated that most of the changes seen in microglia at PND14 and PND28 are due to an alteration in transcriptional activity of PU.1, Creb1, Sp1, and RelA. Fourth, microglia isolated at PND28 from BDS mice showed a high rate of phagocytic activity and reduced expression of many developmental genes, suggesting that BDS impairs the normal maturation of these cells in the developing hippocampus. The generalizability of these findings to other paradigms of postnatal stress and their contribution to abnormal neurodevelopment and behavior need further investigation.

Supplementary Material

Refer to Web version on PubMed Central for supplementary material.

Acknowledgments

References

Bellavance MA, Rivest S. The HPA - immune axis and the immunomodulatory actions of glucocorticoids in the brain. Front. Immunol. 2014; 5:136. [PubMed: 24744759]

Bhatt A, Fan LW, Pang Y. Strategies for myelin regeneration: lessons learned from development. Neural Regener. Res. 2014; 9:1347–1350.

Bilbo SD, Newsum NJ, Sprunger DB, Watkins LR, Rudy JW, Maier SF. Differential effects of neonatal handling on early life infection-induced alterations in cognition in adulthood. Brain Behav. Immun. 2007; 21:332–342. [PubMed: 17126527]

Bolton JL, Huff NC, Smith SH, Mason SN, Foster WM, Auten RL, Bilbo SD. Maternal stress and effects of prenatal air pollution on offspring mental health outcomes in mice. Environ. Health Perspect. 2013; 121:1075–1082. [PubMed: 23823752]

Bredy TW, Grant RJ, Champagne DL, Meaney MJ. Maternal care influences neuronal survival in the hippocampus of the rat. Eur. J. Neurosci. 2003; 18:2903–2909. [PubMed: 14656341]

Butovsky O, Jedrychowski MP, Moore CS, Cialic R, Lanser AJ, Gabriely G, Koeglsperger T, Dake B, Wu PM, Doykan CE, Fanek Z, Liu L, Chen Z, Rothstein JD, Ransohoff RM, Gygi SP, Antel JP,

Weiner HL. Identification of a unique TGF-beta-dependent molecular and functional signature in microglia. Nat. Neurosci. 2014; 17:131–143. [PubMed: 24316888]

Butovsky O, Ziv Y, Schwartz A, Landa G, Talpalar AE, Pluchino S, Martino G, Schwartz M. Microglia activated by IL-4 or IFN-gamma differentially induce neurogenesis and oligodendrogenesis from adult stem/progenitor cells. Mol. Cell. Neurosci. 2006; 31:149–160. [PubMed: 16297637]

Carrion VG, Haas BW, Garrett A, Song S, Reiss AL. Reduced hippocampal activity in youth with posttraumatic stress symptoms: an FMRI study. J. Pediatr. Psychol. 2010; 35:559–569. [PubMed: 19995868]

Chamak B, Morandi V, Mallat M. Brain macrophages stimulate neurite growth and regeneration by secreting thrombospondin. J. Neurosci. Res. 1994; 38:221–233. [PubMed: 8078107]

Champagne DL, Bagot RC, van Hasselt F, Ramakers G, Meaney MJ, de Kloet ER, Joels M, Krugers H. Maternal care and hippocampal plasticity: evidence for experience-dependent structural plasticity, altered synaptic functioning, and differential responsiveness to glucocorticoids and stress. J. Neurosci. 2008; 28:6037–6045. [PubMed: 18524909]

Chugani DC, Muzik O, Juhasz C, Janisse JJ, Ager J, Chugani HT. Postnatal maturation of human GABAA receptors measured with positron emission tomography. Ann. Neurol. 2001a; 49:618–626. [PubMed: 11357952]

Chugani HT, Behen ME, Muzik O, Juhasz C, Nagy F, Chugani DC. Local brain functional activity following early deprivation: a study of postinstitutionalized Romanian orphans. Neuroimage. 2001b; 14:1290–1301. [PubMed: 11707085]

Coelho R, Viola TW, Walss-Bass C, Brietzke E, Grassi-Oliveira R. Childhood maltreatment and inflammatory markers: a systematic review. Acta Psychiatr. Scand. 2014; 129:180–192. [PubMed: 24205846]

Cunningham CL, Martinez-Cerdeno V, Noctor SC. Microglia regulate the number of neural precursor cells in the developing cerebral cortex. J. Neurosci. 2013; 33:4216–4233. [PubMed: 23467340]

Dalmau I, Finsen B, Zimmer J, Gonzalez B, Castellano B. Development of microglia in the postnatal rat hippocampus. Hippocampus. 1998; 8:458–474. [PubMed: 9825958]

Diz-Chaves Y, Astiz M, Bellini MJ, Garcia-Segura LM. Prenatal stress increases the expression of proinflammatory cytokines and exacerbates the inflammatory response to LPS in the hippocampal formation of adult male mice. Brain Behav. Immun. 2013; 28:196–206. [PubMed: 23207108]

Diz-Chaves Y, Pernia O, Carrero P, Garcia-Segura LM. Prenatal stress causes alterations in the morphology of microglia and the inflammatory response of the hippocampus of adult female mice. J. Neuroinflammation. 2012; 9:71. [PubMed: 22520439]

Eaton SL, Roche SL, Llavero Hurtado M, Oldknow KJ, Farquharson C, Gillingwater TH, Wishart TM. Total protein analysis as a reliable loading control for quantitative fluorescent Western blotting. PLoS ONE. 2013; 8:e72457. [PubMed: 24023619]

Erblich B, Zhu L, Etgen AM, Dobrenis K, Pollard JW. Absence of colony stimulation factor-1 receptor results in loss of microglia, disrupted brain development and olfactory deficits. PLoS ONE. 2011; 6:e26317. [PubMed: 22046273]

Faulkner RL, Low LK, Cheng HJ. Axon pruning in the developing vertebrate hippocampus. Dev. Neurosci. 2007; 29:6–13. [PubMed: 17148945]

Feng R, Desbordes SC, Xie H, Tillo ES, Pixley F, Stanley ER, Graf T. PU.1 and C/EBPalpha/beta convert fibroblasts into macrophage-like cells. Proc. Natl. Acad. Sci. U.S.A. 2008; 105:6057–6062. [PubMed: 18424555]

Frank MG, Watkins LR, Maier SF. Stress-and glucocorticoid-induced primingof neuroinflammatory responses: potential mechanisms of stress-induced vulnerability to drugs of abuse. Brain Behav. Immun. 2011; 25(Suppl 1):S21–S28. [PubMed: 21256955]

Garofalo R. Cytokines in human milk. J. Pediatr. 2010; 156:S36–S40. [PubMed: 20105664]

Garrett AS, Carrion V, Kletter H, Karchemskiy A, Weems CF, Reiss A. Brain activation to facial expressions in youth with PTSD symptoms. Depress Anxiety. 2012; 29:449–459. [PubMed: 22553009]

Ghosh S, Geahlen RL. Stress granules modulate SYK to cause microglial cell dysfunction in Alzheimer's Disease. EBioMedicine. 2015; 2:1785–1798. [PubMed: 26870803]

Gomez-Gonzalez B, Escobar A. Prenatal stress alters microglial development and distribution in postnatal rat brain. Acta Neuropathol. 2010; 119:303–315. [PubMed: 19756668]

Hao S, Dey A, Yu X, Stranahan AM. Dietary obesity reversibly induces synaptic stripping by microglia and impairs hippocampal plasticity. Brain Behav. Immun. 2016; 51:230–239. [PubMed: 26336035]

Helmeke C, Ovtscharoff W Jr, Poeggel G, Braun K. Juvenile emotional experience alters synaptic inputs on pyramidal neurons in the anterior cingulate cortex. Cereb. Cortex. 2001; 11:717–727. [PubMed: 11459761]

Herringa RJ, Birn RM, Ruttle PL, Burghy CA, Stodola DE, Davidson RJ, Essex MJ. Childhood maltreatment is associated with altered fear circuitry and increased internalizing symptoms by late adolescence. Proc. Natl. Acad. Sci. U.S.A. 2013; 110:19119–19124. [PubMed: 24191026]

Hess J, Denenberg VH, Zarrow MX, Pfeifer D. Modification of the corticosterone response curve as a function of handling in infancy. Physiol. Behav. 1969; 4:109–111.

Hodes GE, Pfau ML, Leboeuf M, Golden SA, Christoffel DJ, Bregman D, Rebusi N, Heshmati M, Aleyasin H, Warren BL, Lebonte B, Horn S, Lapidus KA, Stelzhammer V, Wong EH, Bahn S, Krishnan V, Bolanos-Guzman CA, Murrough JW, Merad M, Russo SJ. Individual differences in the peripheral immune system promote resilience versus susceptibility to social stress. Proc. Natl. Acad. Sci. U.SA. 2014; 111:16136–16141.

Ivy AS, Rex CS, Chen Y, Dube C, Maras PM, Grigoriadis DE, Gall CM, Lynch G, Baram TZ. Hippocampal dysfunction and cognitive impairments provoked by chronic early-life stress involve excessive activation of CRH receptors. J. Neurosci. 2010; 30:13005–13015. [PubMed: 20881118]

Jackowski A, Perera TD, Abdallah CG, Garrido G, Tang CY, Martinez J, Mathew SJ, Gorman JM, Rosenblum LA, Smith EL, Dwork AJ, Shungu DC, Kaffman A, Gelernter J, Coplan JD, Kaufman J. Early-life stress, corpus callosum development, hippocampal volumetrics, and anxious behavior in male nonhuman primates. Psychiatry Res. 2011; 192:37–44. [PubMed: 21377844]

Johnson JD, Campisi J, Sharkey CM, Kennedy SL, Nickerson M, Greenwood BN, Fleshner M. Catecholamines mediate stress-induced increases in peripheral and central inflammatory cytokines. Neuroscience. 2005; 135:1295–1307. [PubMed: 16165282]

Kaffman A, Krystal JH. New frontiers in animal research of psychiatric illness. Methods Mol. Biol. 2012; 829:3–30. [PubMed: 22231804]

Kaur C, Wu CH, Wen CY, Ling EA. The effects of subcutaneous injections of glucocorticoids on amoeboid microglia in postnatal rats. Arch. Histol. Cytol. 1994; 57:449–459. [PubMed: 7734174]

Kierdorf K, Erny D, Goldmann T, Sander V, Schulz C, Perdiguero EG, Wieghofer P, Heinrich A, Riemke P, Holscher C, Muller DN, Luckow B, Brocker T, Debowski K, Fritz G, Opdenakker G, Diefenbach A, Biber K, Heikenwalder M, Geissmann F, Rosenbauer F, Prinz M. Microglia emerge from erythromyeloid precursors via Pu.1- and Irf8-dependent pathways. Nat. Neurosci. 2013; 16:273–280. [PubMed: 23334579]

Kritas SK, Saggini A, Cerulli G, Caraffa A, Antinolfi P, Pantalone A, Rosati M, Tei M, Speziali A, Saggini R, Conti P. Corticotropin-releasing hormone, microglia and mental disorders. Int. J. Immunopathol. Pharmacol. 2014; 27:163–167. [PubMed: 25004828]

Lenz KM, McCarthy MM. A starring role for microglia in brain sex differences. Neuroscientist. 2015; 21:306–321. [PubMed: 24871624]

Lenz KM, Nugent BM, Haliyur R, McCarthy MM. Microglia are essential to masculinization of brain and behavior. J. Neurosci. 2013; 33:2761–2772. [PubMed: 23407936]

Levine S, Haltmeyer G, Karas G, Denenberg VH. Physiological and behavioral effects of infantile stimulation. Physiol. Behav. 1967; 2:55–59.

Liu D, Diorio J, Day JC, Francis DD, Meaney MJ. Maternal care, hippocampal synaptogenesis and cognitive development in rats. Nat. Neurosci. 2000; 3:799–806. [PubMed: 10903573]

Loi M, Mossink JC, Meerhoff GF, Den Blaauwen JL, Lucassen PJ, Joels M. Effects of early-life stress on cognitive function and hippocampal structure in female rodents. Neuroscience. 2015

Maheu FS, Dozier M, Guyer AE, Mandell D, Peloso E, Poeth K, Jenness J, Lau JY, Ackerman JP, Pine DS, Ernst M. A preliminary study of medial temporal lobe function in youths with a history of caregiver deprivation and emotional neglect. Cog. Affect. Behav. Neurosci. 2010; 10:34–49.

McNamee EN, Griffin EW, Ryan KM, Ryan KJ, Heffernan S, Harkin A, Connor TJ. Noradrenaline acting at beta-adrenoceptors induces expression of IL-lbeta and its negative regulators IL-lra and IL-1RII, and drives an overall anti-inflammatory phenotype in rat cortex. Neuropharmacology. 2010; 59:37–48. [PubMed: 20361987]

Meaney MJ, Aitken DH, Viau V, Sharma S, Sarrieau A. Neonatal handling alters adrenocortical negative feedback sensitivity and hippocampal type II glucocorticoid receptor binding in the rat. Neuroendocrinology. 1989; 50:597–604. [PubMed: 2558328]

Miron VE, Boyd A, Zhao JW, Yuen TJ, Ruckh JM, Shadrach JL, van Wijngaarden P, Wagers AJ, Williams A, Franklin RJ, ffrench-Constant C. M2 microglia and macrophages drive oligodendrocyte differentiation during CNS remyelination. Nat. Neurosci. 2013; 16:1211–1218. [PubMed: 23872599]

Ock J, Lee H, Kim S, Lee WH, Choi DK, Park EJ, Kim SH, Kim IK, Suk K. Induction of microglial apoptosis by corticotropin-releasing hormone. J. Neurochem. 2006; 98:962–972. [PubMed: 16893426]

Pace TW, Wingenfeld K, Schmidt I, Meinlschmidt G, Hellhammer DH, Heim CM. Increased peripheral NF-kappaB pathway activity in women with childhood abuse-related posttraumatic stress disorder. Brain Behav. Immun. 2012; 26:13–17. [PubMed: 21801830]

Paolicelli RC, Bolasco G, Pagani F, Maggi L, Scianni M, Panzanelli P, Giustetto M, Ferreira TA, Guiducci E, Dumas L, Ragozzino D, Gross CT. Synaptic pruning by microglia is necessary for normal brain development. Science. 2011; 333:1456–1458. [PubMed: 21778362]

Paresce DM, Ghosh RN, Maxfield FR. Microglial cells internalize aggregates of the Alzheimer's disease amyloid beta-protein via a scavenger receptor. Neuron. 1996; 17:553–565. [PubMed: 8816718]

Park SD, Cheon SY, Park TY, Shin BY, Oh H, Ghosh S, Koo BN, Lee SK. Intranuclear interactomic inhibition of NF-kappaB suppresses LPS-induced severe sepsis. Biochem. Biophys. Res. Commun. 2015; 464:711–717. [PubMed: 26159927]

Parkhurst CN, Yang G, Ninan I, Savas JN, Yates JR 3rd, Lafaille JJ, Hempstead BL, Littman DR, Can WB. Microglia promote learning-dependent synapse formation through brain-derived neurotrophic factor. Cell. 2013; 155:1596–1609. [PubMed: 24360280]

Pfaffl MW. A new mathematical model for relative quantification in realtime RT-PCR. Nucleic Acids Res. 2001; 29:e45. [PubMed: 11328886]

Poeggel G, Helmeke C, Abraham A, Schwabe T, Friedrich P, Braun K. Juvenile emotional experience alters synaptic composition in the rodent cortex, hippocampus, and lateral amygdala. Proc. Natl. Acad. Sci. U.SA. 2003; 100:16137–16142.

Rice RA, Spangenberg EE, Yamate-Morgan H, Lee RJ, Arora RP, Hernandez MX, Tenner AJ, West BL, Green KN. Elimination of microglia improves functional outcomes following extensive neuronal loss in the hippocampus. J. Neurosci. 2015; 35:9977–9989. [PubMed: 26156998]

Roque A, Ochoa-Zarzosa A, Torner L. Maternal separation activates microglial cells and induces an inflammatory response in the hippocampus of male rat pups, independently of hypothalamic and peripheral cytokine levels. Brain Behav. Immun. 2015

Roy A, Fung YK, Liu X, Pahan K. Up-regulation of microglial CD11b expression by nitric oxide. J. Biol. Chem. 2006; 281:14971–14980. [PubMed: 16551637]

Schafer DP, Lehrman EK, Kautzman AG, Koyama R, Mardinly AR, Yamasaki R, Ransohoff RM, Greenberg ME, Barres BA, Stevens B. Microglia sculpt postnatal neural circuits in an activity and complement-dependent manner. Neuron. 2012; 74:691–705. [PubMed: 22632727]

Smith AM, Gibbons HM, Oldfield RL, Bergin PM, Mee EW, Faull RL, Dragunow M. The transcription factor PU.1 is critical for viability and function of human brain microglia. Glia. 2013; 61:929–942. [PubMed: 23483680]

Spinelli S, Chefer S, Carson RE, Jagoda E, Lang L, Heilig M, Barr CS, Suomi SJ, Higley JD, Stein EA. Effects of early-life stress on serotonin(1A) receptors in juvenile Rhesus monkeys measured by positron emission tomography. Biol. Psychiatry. 2010; 67:1146–1153. [PubMed: 20172506]

Stevens SL, Shaw TE, Dykhuizen E, Lessov NS, Hill JK, Wurst W, Stenzel-Poore MP. Reduced cerebral injury in CRH-R1 deficient mice after focal ischemia: a potential link to microglia and

atrocytes that express CRH-R1. J. Cereb. Blood Flow Metab. 2003; 23:1151–1159. [PubMed: 14526225]

Steward O, Falk PM. Selective localization of polyribosomes beneath developing synapses: a quantitative analysis of the relationships between polyribosomes and developing synapses in the hippocampus and dentate gyrus. J. Comp. Neurol. 1991; 314:545–557. [PubMed: 1814974]

Takatsuru Y, Nabekura J, Ishikawa T, Kohsaka S, Koibuchi N. Early-life stress increases the motility of microglia in adulthood. J. Physiol. Sci. 2015; 65:187–194. [PubMed: 25702174]

Takenouchi T, Nakai M, Iwamaru Y, Sugama S, Tsukimoto M, Fujita M, Wei J, Sekigawa A, Sato M, Kojima S, Kitani H, Hashimoto M. The activation of P2×7 receptor impairs lysosomal functions and stimulates the release of autophagolysosomes in microglial cells. J. Immunol. 2009; 182:2051–2062. [PubMed: 19201858]

Ueno M, Fujita Y, Tanaka T, Nakamura Y, Kikuta J, Ishii M, Yamashita T. Layer V cortical neurons require microglial support for survival during postnatal development. Nat. Neurosci. 2013; 16:543–551. [PubMed: 23525041]

Wakselman S, Bechade C, Roumier A, Bernard D, Triller A, Bessis A. Developmental neuronal death in hippocampus requires the microglial CD11b integrin and DAP12 immunoreceptor. J. Neurosci. 2008; 28:8138–8143. [PubMed: 18685038]

Wang XD, Su YA, Wagner KV, Avrabos C, Scharf SH, Hartmann J, Wolf M, Liebl C, Kuhne C, Wurst W, Holsboer F, Eder M, Deussing JM, Muller MB, Schmidt MV. Nectin-3 links CRHR1 signaling to stress-induced memory deficits and spine loss. Nat. Neurosci. 2013; 16:706–713. [PubMed: 23644483]

Wei L, David A, Duman RS, Anisman H, Kaffman A. Early life stress increases anxiety-like behavior in Balb c mice despite a compensatory increase in levels of postnatal maternal care. Horm. Behav. 2010; 57:396–404. [PubMed: 20096699]

Wei L, Hao J, Kaffman A. Early life stress inhibits expression of ribosomal RNA in the developing hippocampus. PLoS ONE. 2014; 9:e115283. [PubMed: 25517398]

Wei L, Hao J, Lacher RK, Abbott T, Chung L, Colangelo CM, Kaffman A. Early-life stress perturbs key cellular programs in the developing mouse hippocampus. Dev. Neurosci. 2015

Wei L, Meaney MJ, Duman RS, Kaffman A. Affiliative behavior requires juvenile, but not adult neurogenesis. J. Neurosci. 2011; 31:14335–14345. [PubMed: 21976519]

Wei L, Simen A, Mane S, Kaffman A. Early life stress inhibits expression of a novel innate immune pathway in the developing hippocampus. Neuropsychopharmacology. 2012; 37:567–580. [PubMed: 21993208]

Wen AY, Sakamoto KM, Miller LS. The role of the transcription factor CREB in immune function. J. Immunol. 2010; 185:6413–6419. [PubMed: 21084670]

Wohleb ES, Hanke ML, Corona AW, Powell ND, Stiner LM, Bailey MT, Nelson RJ, Godbout JP, Sheridan JF. Beta-Adrenergic receptor antagonism prevents anxiety-like behavior and microglial reactivity induced by repeated social defeat. J. Neurosci. 2011; 31:6277–6288. [PubMed: 21525267]

Wohleb ES, McKim DB, Shea DT, Powell ND, Tarr AJ, Sheridan JF, Godbout JP. Re-establishment of anxiety in stress-sensitized mice is caused by monocyte trafficking from the spleen to the brain. Biol. Psychiatry. 2014; 75:970–981. [PubMed: 24439304]

Wohleb ES, Powell ND, Godbout JP, Sheridan JF. Stress-induced recruitment of bone marrow-derived monocytes to the brain promotes anxiety-like behavior. J. Neurosci. 2013; 33:13820–13833. [PubMed: 23966702]

Wu CH, Chien HF, Chang CY, Chen SH, Huang YS. Response of amoeboid and differentiating ramified microglia to glucocorticoids in postnatal rats: a lectin histochemical and ultrastructural study. Neurosci. Res. 2001; 40:235–244. [PubMed: 11448515]

Yeamans C, Wang D, Paz-Priel I, Torbett BE, Tenen DG, Friedman AD. C/EBPalpha binds and activates the PU.1 distal enhancer to induce monocyte lineage commitment. Blood. 2007; 110:3136–3142. [PubMed: 17671233]
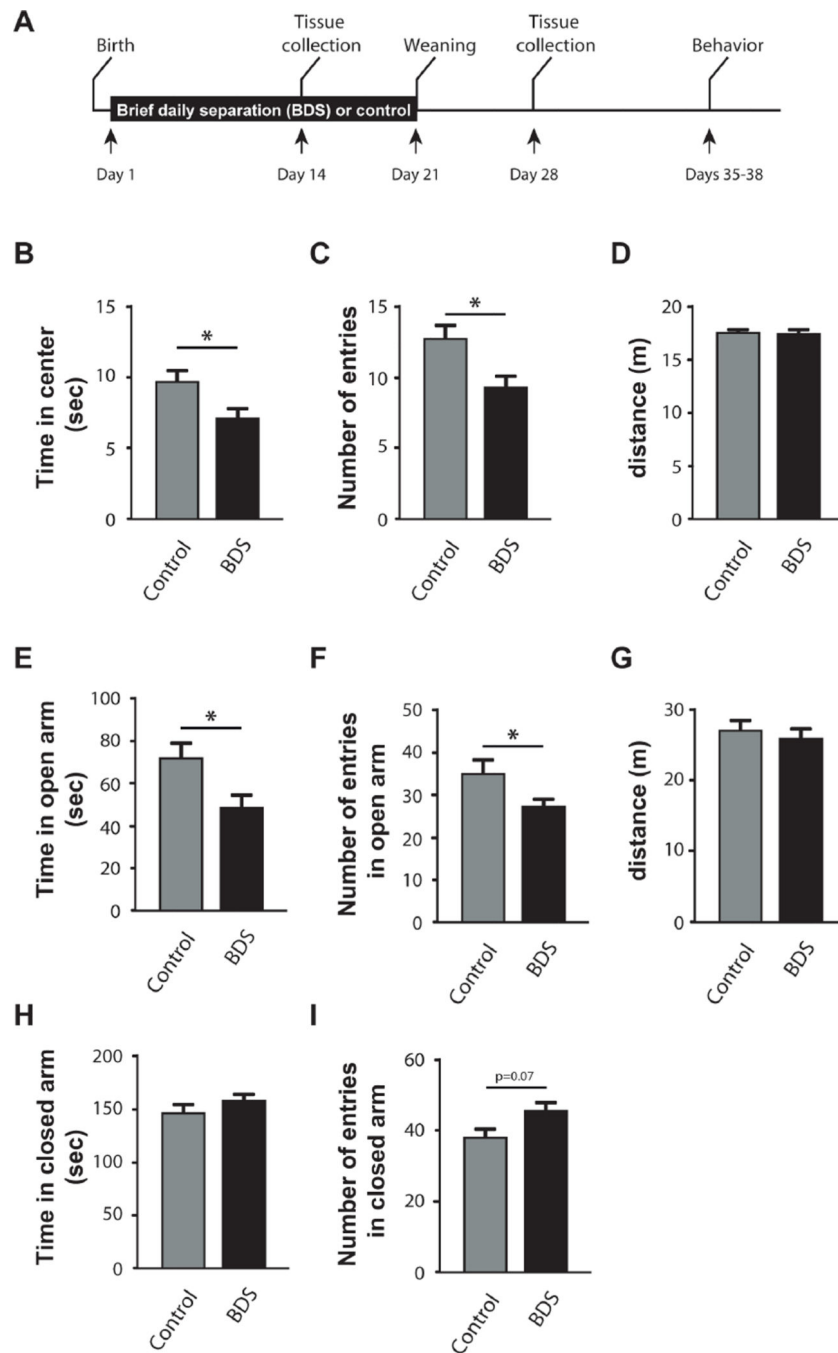
Fig. 1.
BDS increases anxiety-like behavior in juvenile mice. (A) Experimental timeline. Exposure to BDS reduced the time spent in the center (B), and the number of entries into the center of the arena (C), but did not affect the total distance travelled (D) in the open field. BDS mice also spent less time (E) and entered less frequently into the open arms of the elevated plus maze (F). Also shown is the total distance travelled in the elevated plus maze (G), time spent in the closed arms (H), and the number of entries into the closed arms (I) of the elevated plus

maze. Control: N = 21, BDS: N = 23–25, male mice, PND35-38 from 7 to 8 different litters per group. Error bars represent mean ± SEM. *p < 0.05.
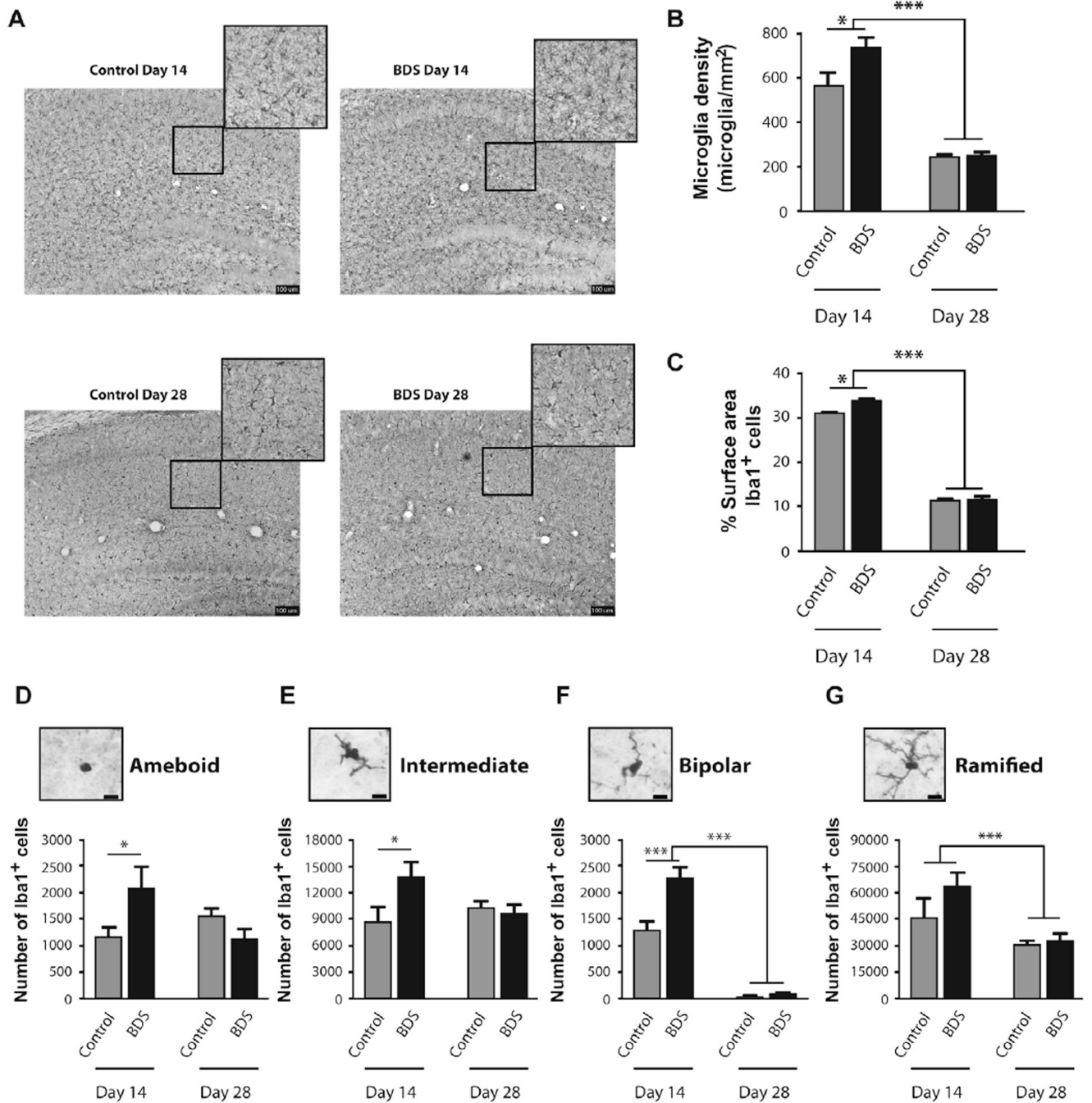
Fig. 2.
BDS causes microgliosis in the hippocampus of 14-day old pups. (A) Representative pictures of Iba-1 staining microglia in the hippocampus of control and BDS male mice at PND14 and PND28. Exposure to BDS increased the density (B), and surface area (C) of microglia present in the hippocampus of 14-day old mice, an effect that did not persist at PND28. BDS caused a significant increase in the number of amoeboid (D), intermediate (E), and bipolar (F) microglia in the hippocampus at PND14, but not PND28. There was a significant effect of age, and a trend (p = 0.099) for the effect of BDS, on the number of

ramified cells (G) in the hippocampus. N = 8–11 mice from 7 to 8 different litters per group. Scale bars in A are 100 μm and 10 μm in D–G, Error bars represent mean ± SEM. *p < 0.05, **p < 0.001.
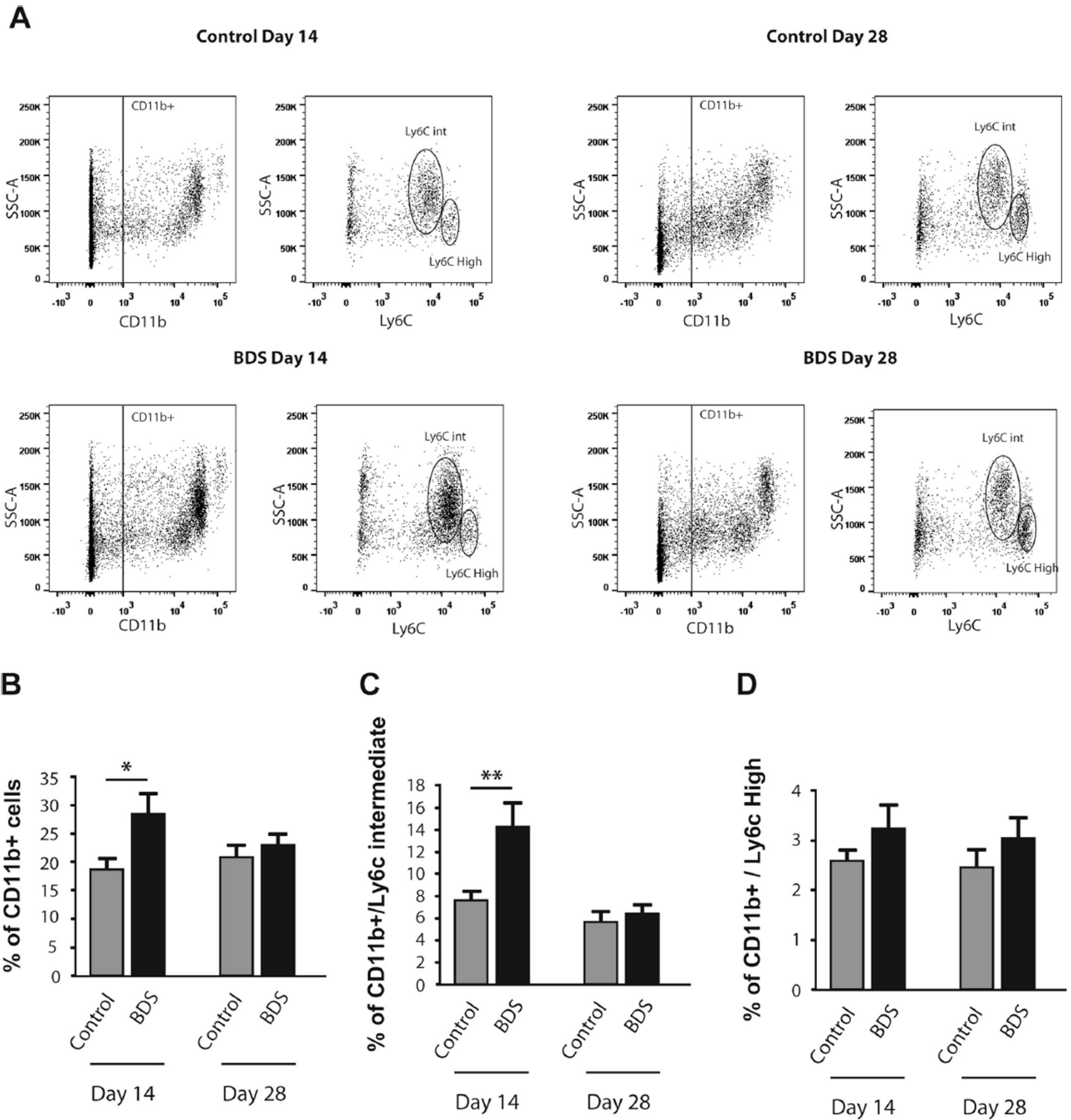
Fig. 3.
BDS increases the number of CD11b-positive cells in the blood of PND14, but not PND28 mice. (A) Representative bivariate dot plots of SSC-A/CD11b (CD11b-positive cells) and SSC-A/Ly6C (granulocytes and monocytes) labeling of blood cells obtained on PND14 and PND28. Gating for CD11b/SSC^{hi}/Ly6C^{int} (granulocytes) and CD11b/SSC^{low}/Ly6C^{hi} (monocytes) is shown on the SSC-A/Ly6c dot plots. BDS increased the total number of CD11b-positive cells (B) and CD11b/SSC^{hi}/Ly6C^{int}-granulocytes (C) at PND14, but not PND28. There was no effect of age or BDS on the percentage of CD11b/SSC^{low}/Ly6C^{hi}

monocytes (D). N = 7–10 mice, from 7 to 8 different litters, per group. Error bars represent mean ± SEM. *p < 0.05, **p < 0.01.
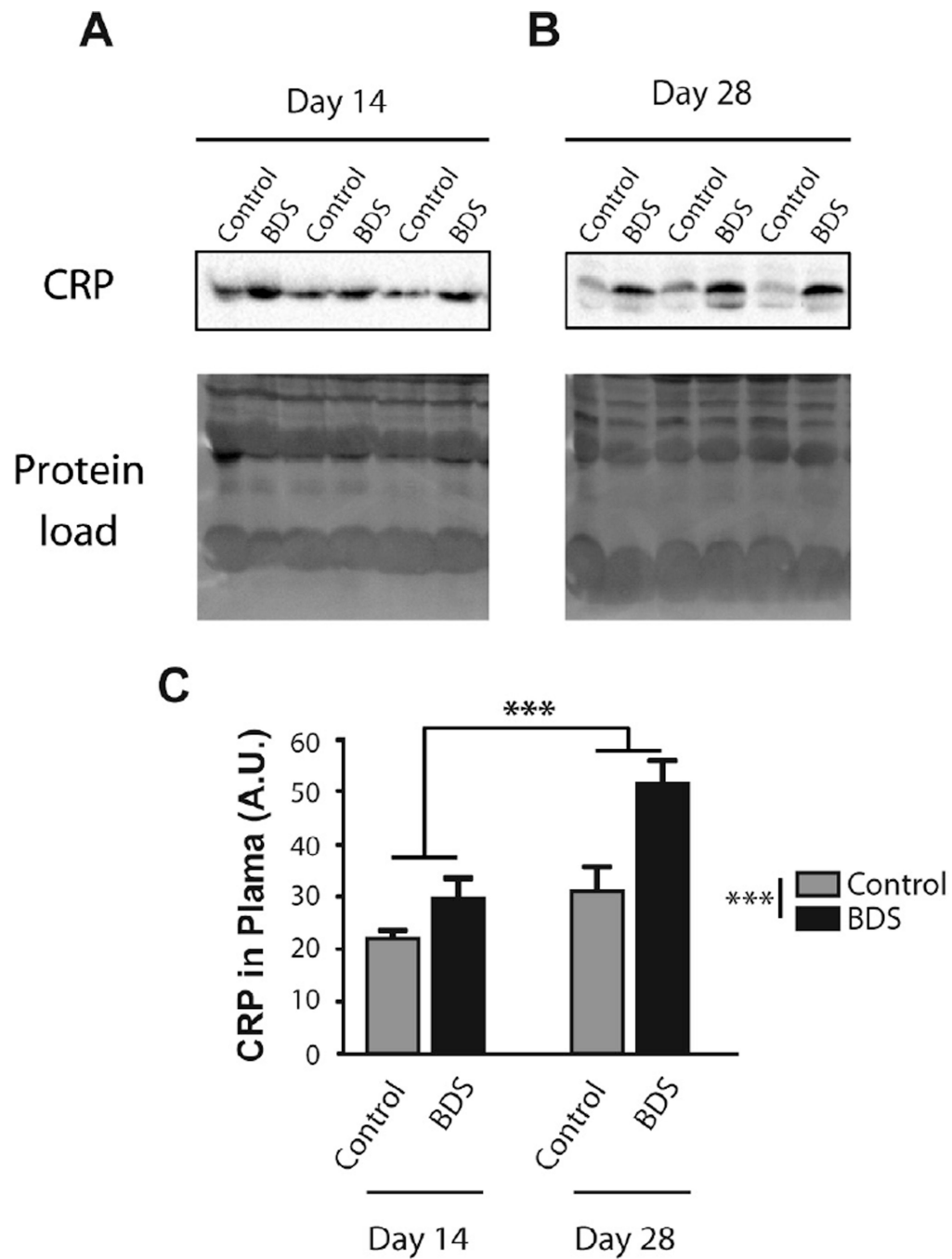
Fig. 4.
Exposure to BDS increases plasma c-reactive protein (CRP) levels in PND14 and PND28 mice. Western blot gels showing levels of CRP in the plasma of PND14 (A) and PND28 (B) mice. Equal protein loading is shown at the bottom (Protein Load) and is the image of activated fluorescent proteins detected by the Stain-Free Gel. (C) Quantification Western blots. Error bars represent mean ± SEM. ***$p < 0.0005$. N = 7–8 mice in each group.
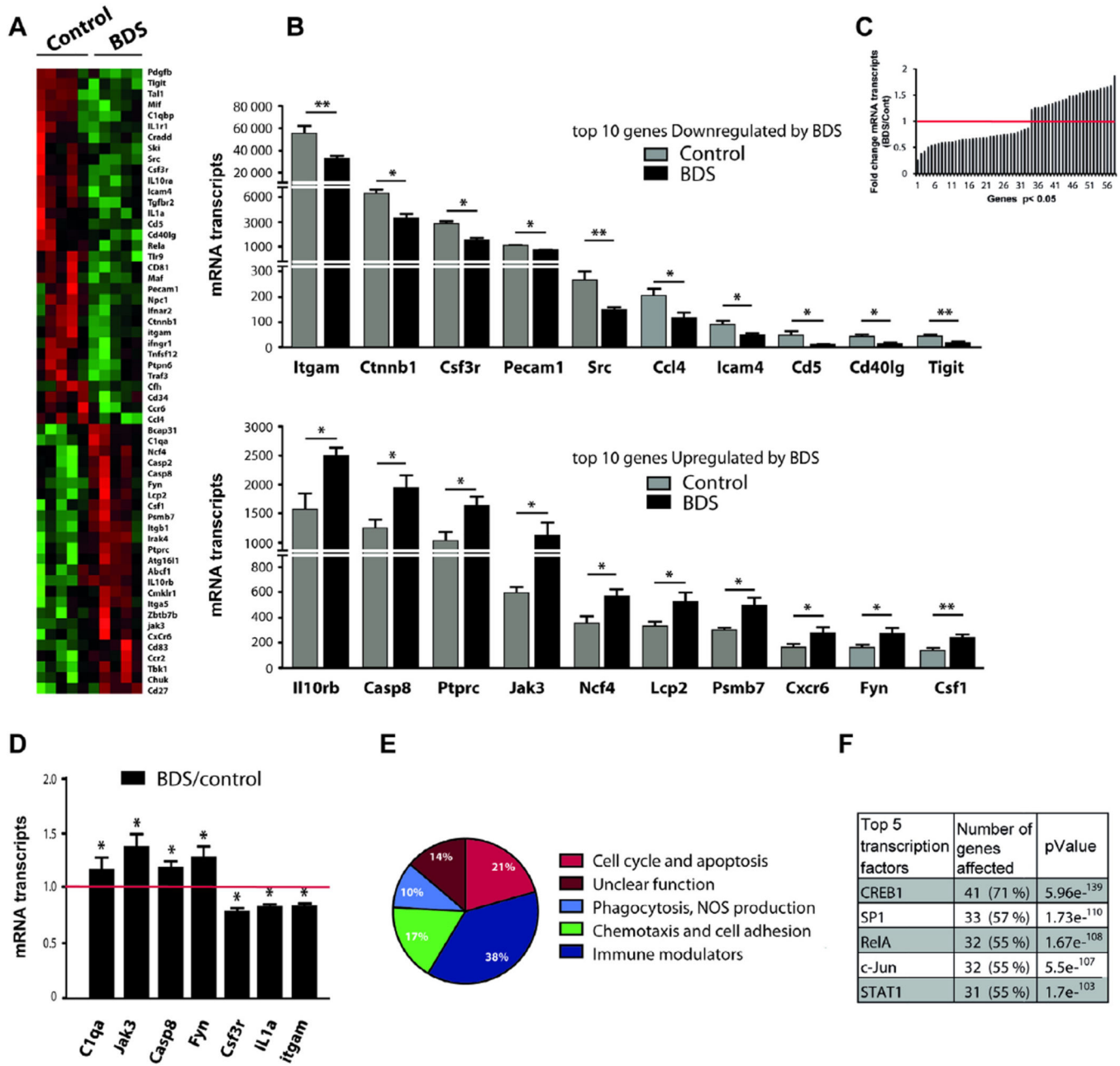
Fig. 5.
Microglial molecular signature is dysregulated in the hippocampus of 14-day old BDS mice. (A) Heat map showing differential gene expression in microglia isolated from the hippocampus of 14-day old mice (green and red color indicate low and high expression respectively). (B) Top: 10 most down-regulated genes, bottom: 10 most up-regulated genes affected by BDS at PND14. (C) Histogram showing the fold change (BDS/Control) for the 58 genes that were differentially regulated by BDS at PND14. (D) q-PCR confirmation of genes found in the immune panel. (E) Path analysis. (F) Promoter analysis. N = 5 mice, from 5 different litters, per group. (For interpretation of the references to color in this figure legend, the reader is referred to the web version of this article.)
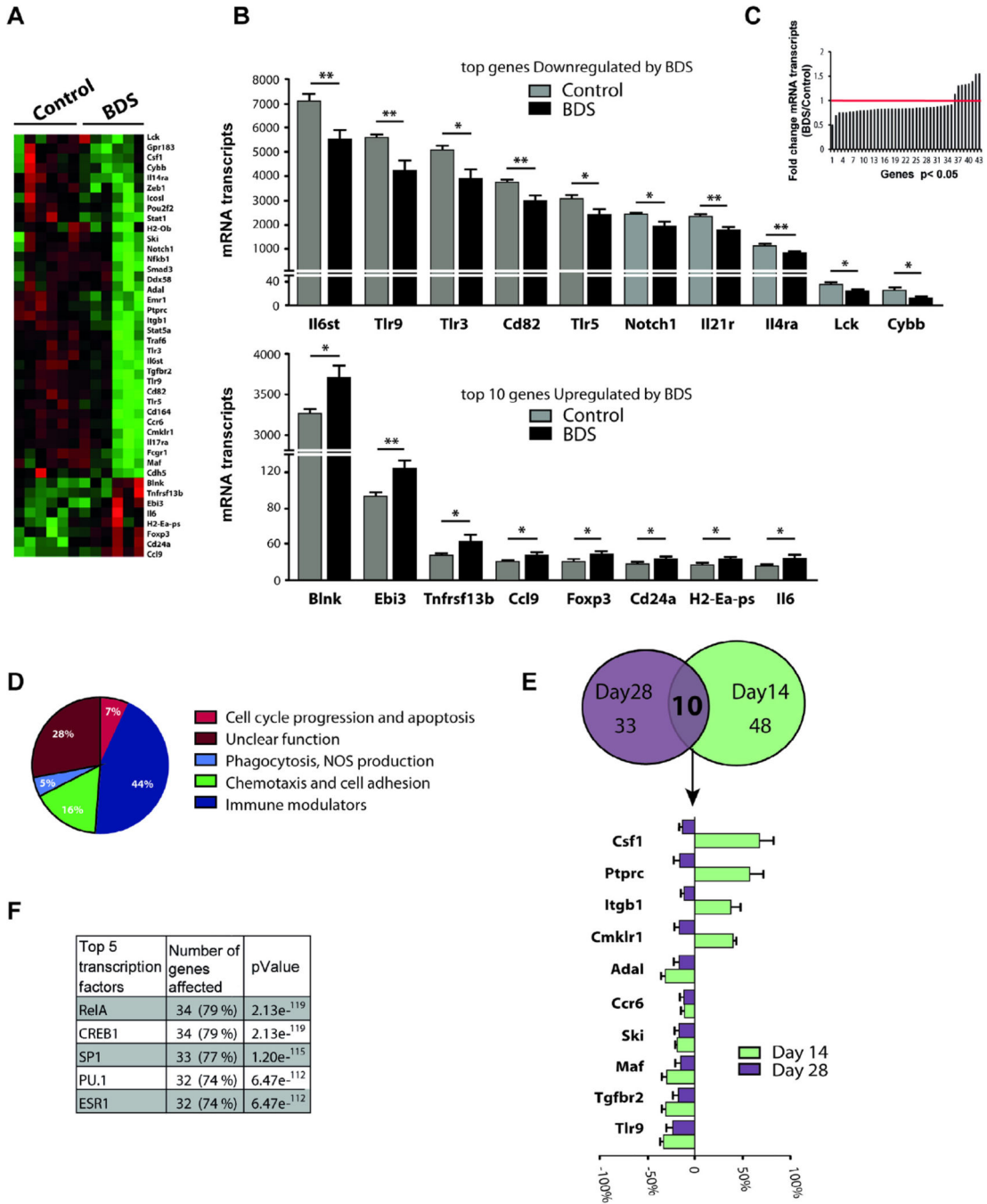
Fig. 6.
BDS alters gene expression in microglia isolated from the hippocampus of PND28 mice. (A) Heat map showing differential gene expression in microglia isolated from the hippocampus of 28-day old male mice (green and red color indicate low and high expression respectively). (B) Top: 10 most down-regulated genes, bottom: only 8 genes were upregulated by BDS at PND28. (C) Histogram showing the fold change (BDS/Control) for the 43 genes that were differentially regulated by BDS on PND28. (D) Path analysis. (E) Ten genes were regulated by BDS on both PND14 and PND28. (F) Promoter analysis. N = 6 mice, from 6 different
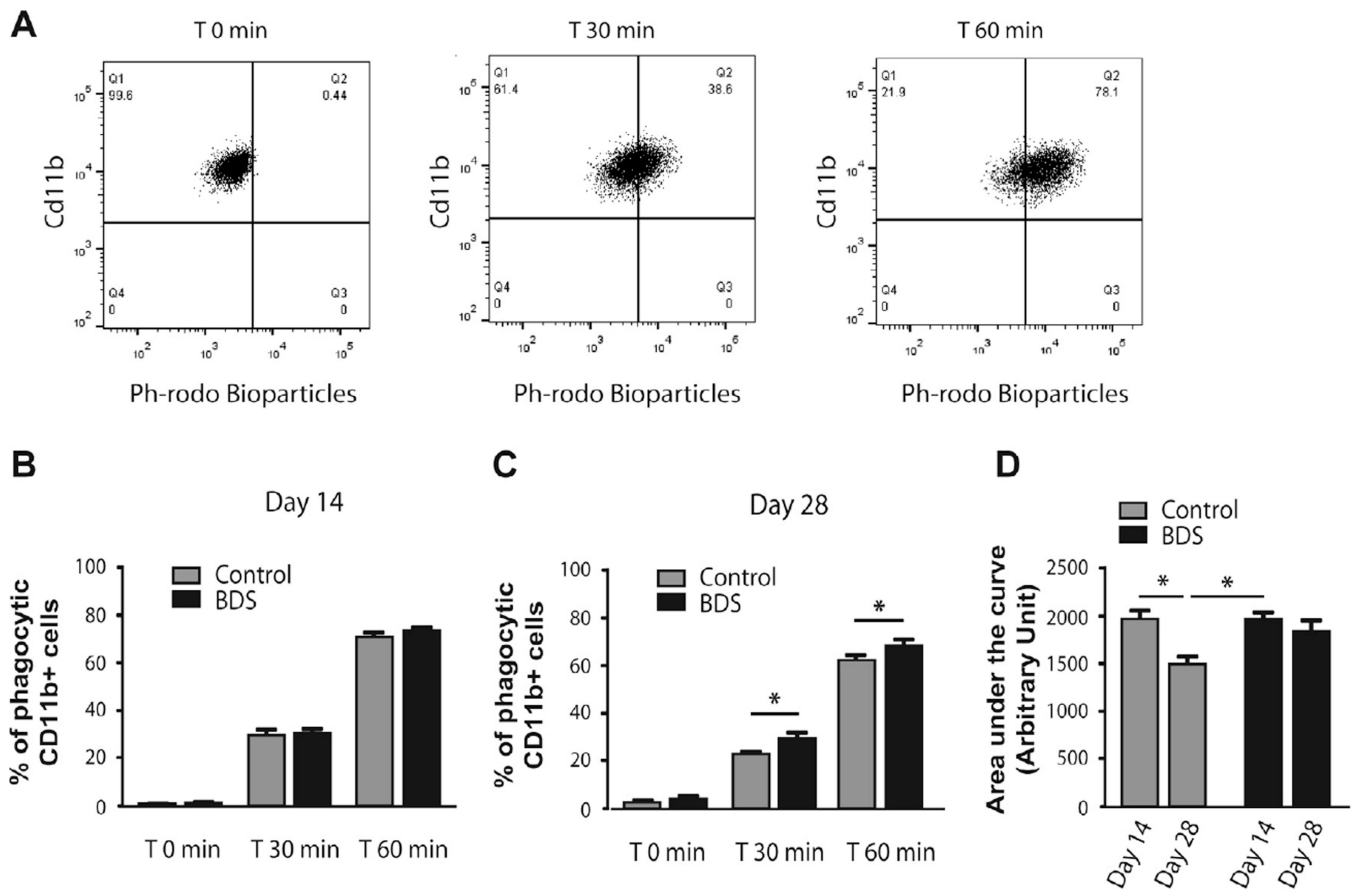
litters, per group. (For interpretation of the references to color in this figure legend, the reader is referred to the web version of this article.)

Fig. 7.
Levels of phagocytic activity decrease with age in control, but not in BDS mice. (A) Time-dependent increase in the uptake of opsonized *E. coli* coated PH-Rhodo-bioparticles in microglia that were acutely isolated from the developing hippocampus. Effects of BDS on *ex-vivo* phagocytic activity in microglia isolated from the hippocampus at PND14 (B) and PND28 (C). (D) Area under the curve (AUC) analysis showing that levels of phagocytic activity decreases across age in controls, but not BDS mice. PND14 (Control n = 12, BDS n = 16), PND28 (Control n = 10, BDS n = 6). Error bars represent mean ± SEM. *p < 0.05, **p < 0.01, ***p < 0.001.
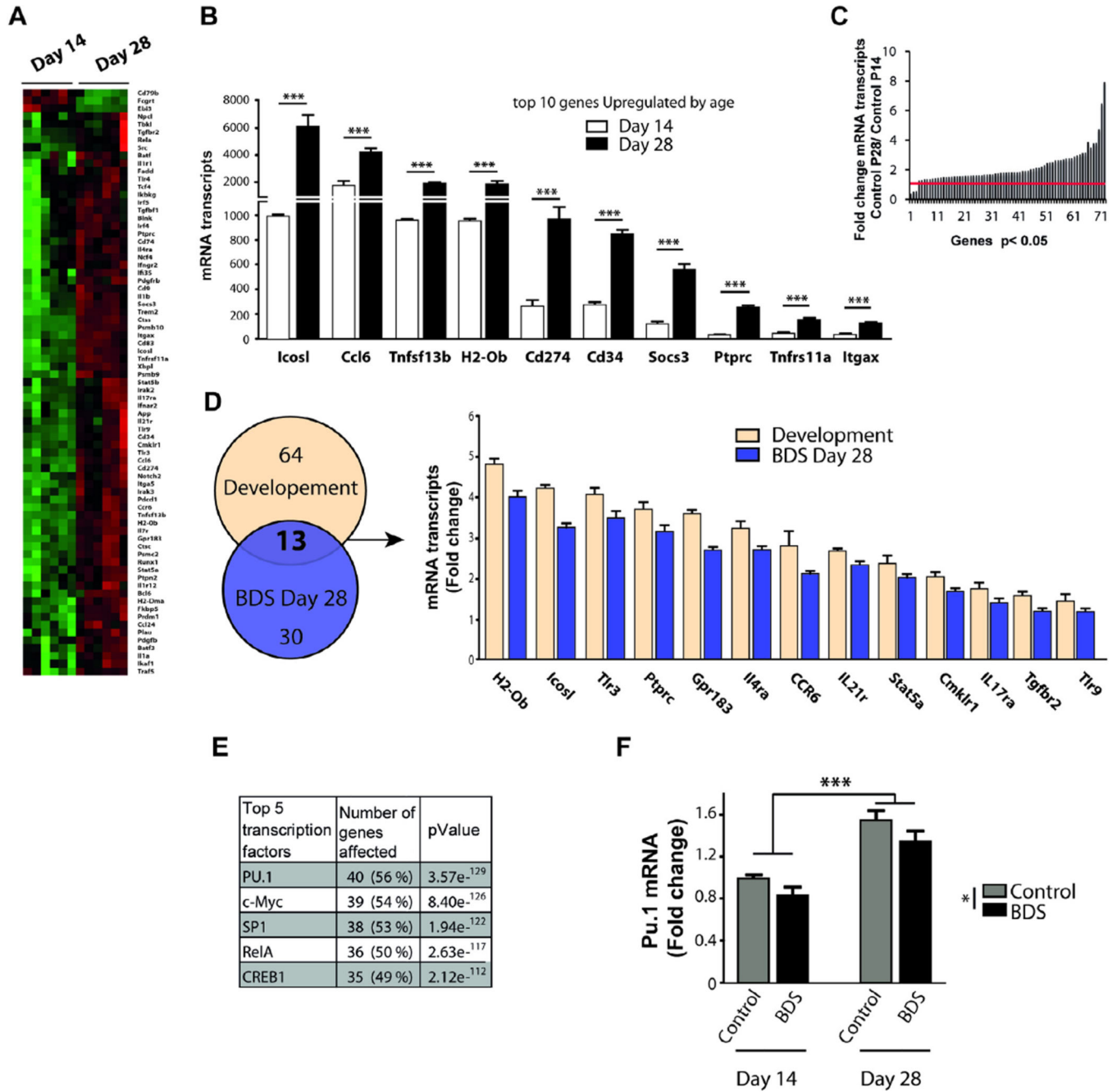
Fig. 8.
BDS perturbs the maturation of microglia in the juvenile hippocampus. (A) Heat-map of developmental genes whose expression changes between PND14 and PND28 in normally developing mice (green and red color indicate low and high expression respectively). (B) Top 10 most upregulated developmental genes. (C) Histogram showing the magnitude of the developmental changes in gene expression between PND14 and PND28 control mice. (D) Genes that are affected by BDS at PND28 and are also developmentally regulated (Y-axis indicates level of expression relative to PND14 control). (E) Promoter analysis. (F) PU.1 is a developmental gene whose expression decreases in BDS mice. (For interpretation of the

references to color in this figure legend, the reader is referred to the web version of this article.)